

INVESTIGATION OF DESALINATION PERFORMANCE OF CAPACITIVE  
DEIONIZATION TECHNOLOGY

A THESIS SUBMITTED TO  
THE GRADUATE SCHOOL OF NATURAL AND APPLIED SCIENCES  
OF  
MIDDLE EAST TECHNICAL UNIVERSITY

BY

SELİN ÖZKUL

IN PARTIAL FULFILLMENT OF THE REQUIREMENTS  
FOR  
THE DEGREE OF MASTER OF SCIENCE  
IN  
ENVIRONMENTAL ENGINEERING

JANUARY 2019



Approval of the thesis:

**INVESTIGATION OF DESALINATION PERFORMANCE OF  
CAPACITIVE DEIONIZATION TECHNOLOGY**

submitted by **SELİN ÖZKUL** in partial fulfillment of the requirements for the degree  
of **Master of Science in Environmental Engineering Department, Middle East  
Technical University** by,

Prof. Dr. Halil Kalıpçılar  
Dean, Graduate School of **Natural and Applied Sciences**

\_\_\_\_\_

Prof. Dr. Bülent İçgen  
Head of Department, **Environmental Eng.**

\_\_\_\_\_

Prof. Dr. İpek İmamoğlu  
Supervisor, **Environmental Eng., METU**

\_\_\_\_\_

Prof. Dr. Hüsnü Emrah Ünalın  
Co-Supervisor, **Met. and Mat. Eng., METU**

\_\_\_\_\_

**Examining Committee Members:**

Prof. Dr. Ayşegül Aksoy  
Environmental Eng., METU

\_\_\_\_\_

Prof. Dr. İpek İmamoğlu  
Environmental Eng., METU

\_\_\_\_\_

Prof. Dr. Hüsnü Emrah Ünalın  
Met. and Mat. Eng., METU

\_\_\_\_\_

Assoc. Prof. Dr. Zarife Göknur Büke  
Material Science and Nanotechnology Eng., TOBB ETÜ

\_\_\_\_\_

Assoc. Prof. Dr. Emrullah Görkem Günbaş  
Chemistry, METU

\_\_\_\_\_

Date: 24.01.2019

**I hereby declare that all information in this document has been obtained and presented in accordance with academic rules and ethical conduct. I also declare that, as required by these rules and conduct, I have fully cited and referenced all material and results that are not original to this work.**

Name, Surname: Selin Özkul

Signature:

## ABSTRACT

### INVESTIGATION OF DESALINATION PERFORMANCE OF CAPACITIVE DEIONIZATION TECHNOLOGY

Özkul, Selin

Master of Science, Environmental Engineering

Supervisor: Prof. Dr. İpek İmamoğlu

Co-Supervisor: Prof. Dr. Hüsnü Emrah Ünalın

January 2019, 84 pages

Capacitive deionization (CDI) is one of the emerging technologies developed with the purpose of water desalination. CDI technology is based on ion electrosorption at the surface of electrically charged electrode couples that are commonly comprised of porous carbon materials. Along with the continuous increase in the global fresh water demand, CDI technology becomes more prominent as an energy efficient and cost-effective water purification process. In this study, ion removal capacity of the CDI process was investigated under various operational conditions using different carbon based electrodes. For this purpose, carbonaceous supercapacitor electrodes were developed from commercially available, cost-effective activated carbon and graphene-like materials, and the use of these materials for deionization was explored in detail. The porosity, morphology and chemical nature of the carbonaceous materials were analysed, and it has been found that both materials are porous with different structural properties. Electrochemical properties of the fabricated electrodes were also investigated, and both electrodes showed good electrochemical reaction kinetics and follow electric double layer mechanism during electrosorption process. Furthermore, deionization performances of the fabricated carbonaceous electrodes were evaluated in a laboratory scale CDI unit. The electrosorption behavior of carbonaceous

electrodes was analyzed at different electrical potentials and water flow rates, and impact of operating parameters on the sorption capacity was investigated. At a flow rate of 20 ml/min and at a potential of 2.0 V, the maximum electrosorptive capacities of 8.9  $\mu\text{mol/g}$  and 10.7  $\mu\text{mol/g}$  were obtained from activated carbon and graphene-like material based electrodes, respectively. In addition, monovalent and divalent ion removal capacities of the fabricated electrodes were determined using solutions with different initial salt concentrations. Graphene-like material with high mesoporosity showed better deionization performance at high concentrations considering removal of both monovalent and divalent ions, yet microporous structured activated carbon reached higher ion removal capacity for monovalent ions at lower salt concentrations.

Keywords: Capacitive Deionization, Electrosorption, Desalination, Ion Removal, Carbon-based Electrodes

## ÖZ

### **KAPASİTİF DEİYONİZASYON TEKNOLOJİSİNİN DESALİNASYON PERFORMANSININ İNCELENMESİ**

Özkul, Selin  
Yüksek Lisans, Çevre Mühendisliği  
Tez Danışmanı: Prof. Dr. İpek İmamoğlu  
Ortak Tez Danışmanı: Prof. Dr. Hüsnü Emrah Ünalın

Ocak 2019, 84 sayfa

Kapasitif deiyonizasyon (CDI) suyun tuzdan arınması amacıyla geliştirilen yeni teknolojilerden birisidir. CDI teknolojisi, genellikle gözenekli karbon malzemelerden üretilen elektrikle yüklü elektrot çiftlerinin yüzeyindeki iyon elektrosorpsiyonuna dayanır. Küresel tatlı su talebindeki sürekli artışla birlikte, CDI teknolojisi enerji tasarruflu ve düşük maliyetli bir su arıtma prosesi olarak daha da öne çıkmaktadır. Bu çalışmada, CDI prosesinin iyon giderme kapasitesi, farklı karbon bazlı elektrotlar kullanılarak çeşitli çalışma koşulları altında incelenmiştir. Bu amaçla, ticari olarak temin edilebilen, uygun maliyetli aktif karbon ve grafen benzeri malzemelerden karbon bazlı süperkapasitör elektrotlar geliştirilmiş ve bu malzemelerin deiyonizasyon için kullanımı detaylı bir şekilde araştırılmıştır. Karbon malzemelerin por yapısı, morfolojisi ve kimyasal yapısı analiz edilmiş ve her iki karbon malzemesinin de farklı yapısal özelliklere sahip gözenekli bir yapıda olduğu belirlenmiştir. Üretilen elektrotların elektrokimyasal özellikleri de incelenmiş, her iki elektrot da iyi elektrokimyasal reaksiyon kinetiği göstermiş ve elektrosorpsiyon prosesi sırasında elektriksel çift tabaka mekanizmasını izlemiştir. Ayrıca, üretilen karbon bazlı elektrotların deiyonizasyon performansları laboratuvar ölçekli bir CDI ünitesinde değerlendirilmiştir. Karbon elektrotların elektrosorpsiyon davranışı, farklı

elektrik potansiyellerinde ve su akış hızlarında analiz edilmiş, ve çalışma parametrelerinin sorpsiyon kapasitesi üzerindeki etkisi belirlenmiştir. 20 ml/dak akış hızında ve 2.0 V potansiyelde, aktif karbon ve grafen benzeri malzeme bazlı elektrotlarının sırasıyla 8.9  $\mu\text{mol/g}$  ve 10.7  $\mu\text{mol/g}$  maksimum elektrosorptif kapasite değerleri elde edilmiştir. Ek olarak, üretilen elektrotların tek ve iki değerli iyon giderim kapasiteleri, farklı başlangıç tuz konsantrasyonlarına sahip çözeltiler kullanılarak incelenmiştir. Yüksek mezopor oranına sahip olan grafen benzeri malzeme, hem tek hem de iki değerli iyonların giderimi göz önüne alındığında yüksek konsantrasyonlarda daha iyi deiyonizasyon performansı göstermiştir, ancak mikropor yapılı aktif karbon, düşük tuz konsantrasyonlarında tek değerlikli iyonlar için daha yüksek iyon giderim kapasitesine ulaşmıştır.

Anahtar Kelimeler: Kapasitif Deiyonizasyon, Elektrosorpsiyon, Tuzsuzlaştırma, İyon Giderimi, Karbon-bazlı Elektrotlar

To my mother Ülkü Akpulat...

## ACKNOWLEDGMENTS

The supervisor of this thesis was Assist. Prof. Dr. Derya Dursun Balcı until the time she left METU in September, 2017. Following that, Prof. Dr. İpek İmamođlu became the supervisor and oversaw the finalization of experimental work and write-up of thesis, with continuing help from Assist. Prof. Dr. Derya Dursun Balcı. I would like to express my deepest gratitude to my supervisor Prof. Dr. İpek İmamođlu and my co-supervisor Prof. Dr. H. Emrah Ünalán for their valuable comments, guidance and support during this study. Also, I would like to express my sincere appreciation to Assist. Prof. Dr. Derya Dursun Balcı for her valuable discussions, contributions and continuous support throughout this thesis. Her guidance helped me in all the time during this study.

I would like to appreciate Dr. Recep Yüksel for his teachings and guidance during my lab work. I also would like to thank Mete Batuhan Durukan for helping me with important analyses, and his friendship and endless support during all period. I owe my special thank to my dearest friends and lab-mates Dođancan Tigan, Şensu Tunca, Sevim Polat Genlik and Ece Alpuđan for their support throughout my study. Also, I would like to thank Dođa Dođanay, Şeyma Koç, İpek Bayraktar, Alptekin Aydınlí, Şahin Coşkun, Merve Nur Güven, Yusuf Tutel and Elif Özlem Güner as great lab-mates. I always feel lucky to be a part of this research group.

I am also thankful to my lifelong friends Elif Tekin and Ođul Can. I deeply appreciate their intimate friendship, great moral support and belief in me. I also would like to thank my friends and colleagues Gizem Yücel, Nazlı Barçın Dođan, Hazal Aksu Bahçeci, Pınar Tuncer, Melike Kiraz and Ceren Ayyıldız for their constant help and support through my thesis study.

I would like to express my special thanks to Bora Okan for his endless love, support and patience during this stressful time period. Thank you for always being by my side whenever I needed.

Lastly, I am deeply grateful to my family; my mother Ülkü Akpulat, my grandmother Kadriye Akpulat, my sister Nil Özkul and Spike for their unconditional love and understanding. Thank you for always being there for me, supporting me and encouraging me to achieve all my wishes. I love you.

I gratefully acknowledge the financial support provided by The Scientific and Technological Research Council of Turkey (TUBITAK) under project grant no: 115Y013 and by the Middle East Technical University with project numbers of BAP-08-11-2015-034 and BAP-03-11-2017-004.

## TABLE OF CONTENTS

ABSTRACT .....	v
ÖZ .....	vii
ACKNOWLEDGMENTS.....	x
TABLE OF CONTENTS.....	xii
LIST OF TABLES.....	xv
LIST OF FIGURES .....	xvi
LIST OF ABBREVIATIONS .....	xviii
CHAPTERS	
1. INTRODUCTION .....	1
1.1. Global Challenge of Fresh Water Supply .....	1
1.2. Conventional Desalination Technologies .....	5
1.3. Motivation and Aim of the Study .....	7
2. LITERATURE REVIEW.....	9
2.1. Capacitive Deionization Technology.....	9
2.2. Working Principles of the CDI Process .....	10
2.3. Historical Development and Current Status of the CDI Technology .....	11
2.4. Advantages and Limitations of the CDI Process.....	13
2.5. Materials Used in CDI Electrodes .....	15
2.5.1. Electrode Active Materials.....	15
2.5.1.1. Carbon Materials .....	16
2.5.1.2. Metal Oxides .....	20
2.5.1.3. Conducting Polymers.....	21

2.5.2.	Conductive Additives .....	23
2.5.3.	Polymer Binders .....	23
2.5.4.	Current Collectors .....	23
2.6.	CDI Process Configurations.....	24
2.6.1.	Unit Cell Geometries .....	24
2.6.2.	Process Operating Systems .....	25
2.7.	CDI Process Operation Parameters .....	27
2.7.1.	Applied Voltage .....	27
2.7.2.	Flow Rate .....	28
2.7.3.	Initial Salt Concentration and Ion Type.....	29
3.	MATERIALS AND METHODS.....	31
3.1.	Preparation of the Lab-scale CDI Unit .....	31
3.2.	Materials Used in the Experiments.....	32
3.3.	Electrode Fabrication.....	33
3.4.	Material Characterizations .....	34
3.4.1.	Scanning Electron Microscopy (SEM) .....	35
3.4.2.	Transmission Electron Microscopy (TEM) .....	35
3.4.3.	Fourier-Transform Infrared (FTIR) Spectroscopy .....	35
3.4.4.	X-Ray Diffraction (XRD) Analysis.....	35
3.4.5.	Raman Spectroscopy .....	35
3.4.6.	Brunauer-Emmett-Teller (BET) Surface Area Analysis .....	36
3.5.	Electrochemical Characterizations .....	36
3.5.1.	Cyclic Voltammetry (CV).....	36
3.5.2.	Galvanostatic Charge Discharge (GCD).....	37

3.6.	Electrosorption Experiments .....	38
3.6.1.	Effect of System Operation Parameters on Electrosorptive Capacity .	41
3.6.2.	Effect of Ion Type and Concentration on Electrosorptive Capacity ...	41
3.6.3.	Regeneration of the Fabricated Electrodes .....	41
4.	RESULTS AND DISCUSSIONS.....	43
4.1.	Characterization of the Materials Used in CDI Electrodes.....	43
4.2.	Characterization of the Fabricated CDI Electrodes .....	47
4.3.	Electrosorption Experiments .....	52
4.3.1.	Effect of Water Flow Rate and Applied Voltage .....	52
4.3.2.	Effect of Ion Type and Concentration in the Feed Water .....	55
4.3.3.	Regeneration of the Fabricated CDI Electrodes.....	59
5.	CONCLUSIONS.....	63
6.	RECOMMENDATIONS FOR FUTURE STUDIES .....	65
	REFERENCES .....	67

## LIST OF TABLES

### TABLES

Table 1.1 Classification of water in terms of the salinity [18].....	2
Table 1.2 TDS limitations for different water applications. ....	4
Table 2.1 Electrosorption capacities of different electrodes used in CDI applications. .....	22
Table 4.1 A comparison of CDI results of this study and similar studies with carbon based electrodes from literature.....	59

## LIST OF FIGURES

### FIGURES

Figure 1.1 Global increase in world population and water consumption [6].	1
Figure 1.2 Global desalination industry share by technology and users [5].	5
Figure 2.1 Schematic description of the CDI process.	9
Figure 2.2 Representation of the electrical double layer and potential distribution.	10
Figure 2.3 The number of studies published in the CDI field since the year 2000 [43].	12
Figure 2.4 Timeline of the materials used in CDI electrodes: (a) activated carbon [54], (b) carbon aerogel [7], (c) metal oxide [55], (d) carbon nanotube [7], (e) mesoporous carbon [7], (f) graphene [56].	16
Figure 2.5 The most widely used CDI system configurations; (a) Flow-by mode, (b) Flow-through mode, (c) Electrostatic ion pumping and (d) Deionization using wire electrodes [7].	25
Figure 3.1 A photograph of the lab-scale CDI unit used in the experiments.	32
Figure 3.2 A photograph of the fabricated electrode.	33
Figure 3.3 Configuration of the CDI unit cell.	34
Figure 3.4 Typical CV curve of a supercapacitor electrode [122].	37
Figure 3.5 Typical GCD curve of a supercapacitor electrode [123].	38
Figure 3.6 Illustration of the laboratory scale CDI system used in the experiments.	39
Figure 3.7 Concentration vs conductivity calibration graphs of the (a) NaCl and (b) CaCl <sub>2</sub> salts used in the CDI experiments.	40
Figure 4.1 SEM images of (a) AC powder and (b) GLM used in the CDI electrodes.	43
Figure 4.2 (a) Low magnification and (b) high magnification TEM images and (c) FTIR spectrum and (d) XRD pattern of the GLM used in the CDI electrodes.	44
Figure 4.3 Raman spectra of AC powder and GLM used in the fabrication of CDI electrodes.	45

Figure 4.4 (a) Nitrogen adsorption-desorption isotherms and (b) pore size distributions of the AC powder and GLM used for the CDI electrodes. ....	46
Figure 4.5 SEM images of the (a) AC and (b) GLM based freshly prepared (non-used) electrodes. Insets show the cross-sectional images of the electrodes. ....	47
Figure 4.6 CV analysis results for AC and GLM based electrodes using voltage windows of (a,b) 1.6 V, (c,d) 1.8 V and (e,f) 2.0 V, respectively. ....	48
Figure 4.7 CV analysis results for (a) AC and (b) GLM based electrodes using a scan rate of 50 mV and varying voltage windows. ....	49
Figure 4.8 Comparative CV analysis results for AC and GLM based electrodes using 50 mV scan rate and 0 - 2.0 V voltage window. ....	49
Figure 4.9 GCD analysis results for AC and GLM based electrodes at different voltages of (a,b) 1.6 V, (c,d) 1.8 V and (e,f) 2.0 V, respectively. ....	50
Figure 4.10 Calculated specific capacitance values of the fabricated electrodes with respect to applied currents of 50, 75 and 100 mA and at 0 - 2.0 V voltage window. ....	51
Figure 4.11 Results of electrosorption experiments for AC and GLM based electrodes at a flow rate of (a,b) 5 ml/min, (c,d) 10 ml/min and (e,f) 20 ml/min. ....	52
Figure 4.12 Average electrosorptive capacities of (a) AC and (b) GLM based electrodes based on different flow rates and applied voltages. ....	53
Figure 4.13 Results of electrosorption experiments for AC and GLM based electrodes using a feed solution salt concentration of (a,b) 50 ppm, (c,d) 100 ppm and (e,f) 200 ppm. ....	55
Figure 4.14 Results of control experiments for (a) AC and (b) GLM based electrodes using DI water as a feed solution. ....	56
Figure 4.15 Average electrosorptive capacities of (a) AC and (b) GLM based electrodes based on different flow rates and applied voltages. ....	57
Figure 4.16 Regeneration test results of the AC and GLM based electrodes, showing: (a, b) all cycles and (c,d) comparison of first and last cycles. ....	60
Figure 4.17 SEM images of the AC and GLM based electrodes (a,b) before and (c,d) following CDI process. Insets show the cross-sectional images of the electrodes. ..	62

## LIST OF ABBREVIATIONS

### ABBREVIATIONS

<b>AC</b>	Activated Carbon
<b>ACC</b>	Activated Carbon Cloth
<b>ATR</b>	Attenuated Total Reflection
<b>BOD</b>	Biological Oxygen Demand
<b>CA</b>	Carbon Aerogel
<b>CaCl<sub>2</sub></b>	Calcium Chloride
<b>CDI</b>	Capacitive Deionization
<b>CNT</b>	Carbon Nanotube
<b>COD</b>	Chemical Oxygen Demand
<b>CV</b>	Cyclic Voltammetry
<b>CVD</b>	Chemical Vapor Deposition
<b>DI</b>	Deionized
<b>EC</b>	Electrosorptive Capacity
<b>ED</b>	Electrodialysis
<b>EDL</b>	Electrical Double Layer
<b>FTIR</b>	Fourier-Transform Infrared
<b>GCD</b>	Galvanostatic Charge Discharge
<b>GLM</b>	Graphene-like Material
<b>GR</b>	Graphene
<b>IR</b>	Internal Resistance
<b>MED</b>	Multi Effect Distillation
<b>MnO<sub>2</sub></b>	Manganese Dioxide
<b>MSF</b>	Multi Stage Flash Distillation
<b>N</b>	Nitrogen
<b>NaCl</b>	Sodium Chloride
<b>OMC</b>	Ordered Mesoporous Carbon
<b>P</b>	Phosphorous

<b>PANI</b>	Polyaniline
<b>ppm</b>	Parts per million
<b>PPy</b>	Polypyrrole
<b>PTFE</b>	Polytetrafluoroethylene
<b>PVDF</b>	Polyvinylidene Fluoride
<b>RO</b>	Reverse Osmosis
<b>SEM</b>	Scanning Electron Microscopy
<b>SnO<sub>2</sub></b>	Tin Oxide
<b>SWCNT</b>	Single-walled Carbon Nanotube
<b>TDS</b>	Total Dissolved Solids
<b>TEM</b>	Transmission Electron Microscopy
<b>TiO<sub>2</sub></b>	Titanium Dioxide
<b>XRD</b>	X-Ray Diffraction
<b>ZnO</b>	Zinc Oxide



# CHAPTER 1

## INTRODUCTION

### 1.1. Global Challenge of Fresh Water Supply

The accessibility of affordable clean water can be considered as one of the important technological, social, and economic challenges of the 21<sup>st</sup> century. Over the past century, world population has tripled while the water demand increased over six times. Growing world population, improved living standards, urbanization, developing modern industry, increasing agricultural activities and global warming lead to continuous increase in the global demand for limited freshwater resources. Agricultural irrigation accounts for the vast majority of global water consumption (70%), followed by industrial (20%) and domestic water use (10%) [1 - 5]. A graph showing world population increase rate in comparison to water consumption is provided in Figure 1.1.

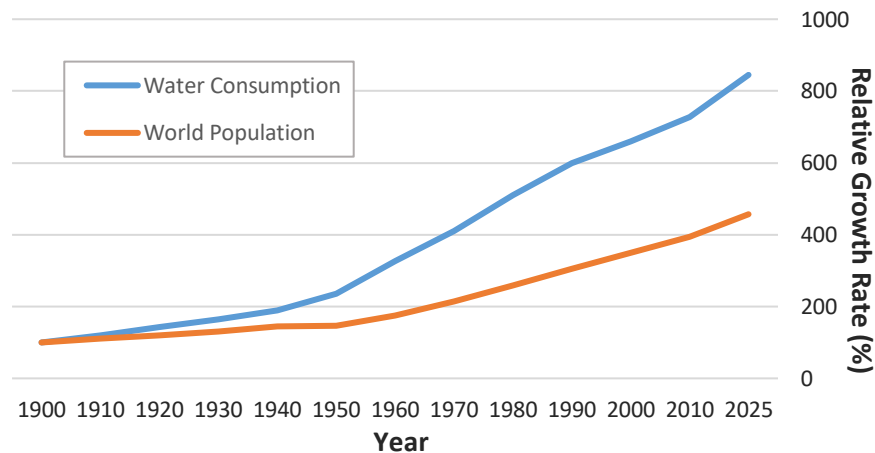


**Figure 1.1** Global increase in world population and water consumption [6].

In addition to increasing water demand, contamination of the available freshwater resources as a result of agricultural, industrial, human activities and discharge of

wastewaters without proper treatment, and excessive withdrawals of groundwater that causes seawater intrusion in wells make most groundwater sources to become unusable as freshwater [7 - 10]. Today, there are 36 countries that do not have sufficient water resources to sustain agriculture and economic development; and more than a billion people do not have access to safe freshwater sources. Also, it is predicted that 2 - 7 billion people would face water scarcity by the year 2050 [10 - 14]. World Resources Institute (WRI) made a study on the future water stress, which is a measure of competition and depletion of surface water, in 167 countries by the year 2040. As a result of this study, it has been found that 33 countries will face extremely high water stress in 2040, including Turkey, which means that these countries will possibly be more vulnerable to water scarcity than they are today [15]. Increase in the global water demand and lack of sufficient resources introduce the need to find new, sustainable and clean freshwater resources.

According to United States Geological Survey (USGS), more than 97% of the natural water resources on the Earth consist of seawater and brackish water, which is unsuitable for irrigation, domestic uses, hydroelectricity generation, industrial uses and for human consumption. Most of the remaining freshwater resources are not available for use and are distributed in glaciers (68.7%) and as groundwater (30.1%). Therefore, only about 0.24% of the Earth's total water supply accounts for available fresh water [16, 17]. Classification of the water bodies in terms of their salinity (total dissolved solids) is given in Table 1.1.

**Table 1.1** Classification of water in terms of the salinity [18].

<b>Classification</b>	<b>Total Dissolved Solids (TDS, ppm)</b>
Freshwater	< 1,000
Brackish water	1,000 - 15,000
Saline water	15,000 - 30,000
Sea water	30,000 - 40,000
Brine	> 40,000

Considering the larger amount of brackish/salty water than that of freshwater in the world, utilizing these various water resources for human consumption in daily, agricultural and industrial use gained significant importance. This is because of freshwater shortage and pollution, which endanger the quality of life on the Earth, especially in arid and semi-arid countries. In today's conditions, the process of removing salt from saline water (desalination) remains as the most reliable, effective and permanent solution to obtain fresh water. In many places that severely suffer from water scarcity, like the Middle East and Singapore, there are no alternative ways to obtain fresh water other than seawater desalination [16, 17, 19]. Currently, Turkey is recognized as a country experiencing water shortage with the amount of water per capita of 1.519 m<sup>3</sup>/year, which is expected to be 1.120 m<sup>3</sup>/year in 2030 [20]. In other words, Turkey will face extreme water stress in the following years and will become a "water-poor" country. Considering that Turkey is mostly surrounded by sea and brackish water resources, desalination might be a favourable solution to overcome water scarcity.

In addition to brackish/sea water desalination, reuse and reclamation of the industrial and municipal wastewater is another way to obtain fresh water. Especially, some industries like food and beverage, chemical, petroleum, textile and leather tanning as well as power plant cooling towers produce wastewater with high salinity. The conventional wastewater treatment processes are able to remove the organic matter (BOD, COD) and nutrients (N, P) from wastewater, but the dissolved salt still remains in the treated effluent. Thus, further treatment is required to remove the salt from treated effluent before re-using it as a valuable reclaimed water [21, 22]. Desalination should therefore be considered as an important process to create alternative fresh water resources.

The high salt content in water causes significant problems and prevents the extensive use of the reclaimed water in many fields. The long term use of high-salinity water for urban and agricultural irrigation leads to accumulation of salt ions (Na<sup>+</sup>, Mg<sup>2+</sup>, Ca<sup>2+</sup>

etc.) in the soil and causes soil alkalization problem [23]. High salt content in the soil causes water deficiency and reduces the ability of plants to acquire water; thus, resulting in dehydration of the plant. Also, some ions, especially  $\text{Cl}^-$ , are toxic to the plants and as the concentration of these ions increases, plants get poisoned. This eventually stops plant reproduction, causes growth reduction or even death of the plants. In addition, using high salinity water in buildings results in the reaction of hard water minerals like  $\text{Ca}^{2+}$  and  $\text{Mg}^{2+}$  with soap anions and decreases the cleaning efficiency. Hence, increases detergent consumption which would lead to economic and environmental issues. These ions also induce corrosion/scaling problems and serious failures in pipelines of boilers, heat exchangers, and electrical appliances such as dishwashers, washing machines, steam irons. They also reduce the service life of these aforementioned appliances [22, 24]. Moreover, high salinity levels may affect the taste of drinking water and pose multiple health risks, including hypertension, kidney failure, gynaecological and gastroenterological diseases [25]. Therefore, salt content should be removed from the water prior to proper applications. In order to minimize its harmful effects, there are limitations for TDS levels in water used in different fields, as shown in Table 1.2.

**Table 1.2** TDS limitations for different water applications.

<b>Purpose of Use</b>		<b>TDS Limitations</b>	<b>Ref</b>
Urban use		< 2,000 ppm	[26]
Agricultural irrigation		< 2,000 ppm	
Industrial use	Steam	0.05 – 1.0 ppm	
	Boiler water	0.05 – 3,500 ppm	
Drinking water		< 600 ppm	[27]

## 1.2. Conventional Desalination Technologies

Currently, various technologies are widely used for desalination and softening applications, such as membrane processes: reverse osmosis (RO), nanofiltration (NF) and electrodialysis (ED); and thermal processes: multi-stage flash distillation (MSF) and multi-effect distillation (MED). In the early 2000s, the worldwide desalination technology share was dominated with a 60% share by thermal processes. Now this situation is shifted to membrane based processes. This is because around 70% of the desalination plants installed after the year 2000 were membrane desalination plants. Today, the RO process is the most commonly used desalination technology, followed by MSF and MED processes. The majority of desalination capacity is owned by municipalities for drinking water supply and industrial utilities for cooling and steam production mostly [5, 17]. Global desalination industry sharings are as shown in Figure 1.2. Seawater desalination accounts for the largest percentage of the total global desalination capacity at around 60%, followed by brackish water at 21%, river/lake water at 8% and wastewater at 6% [28].

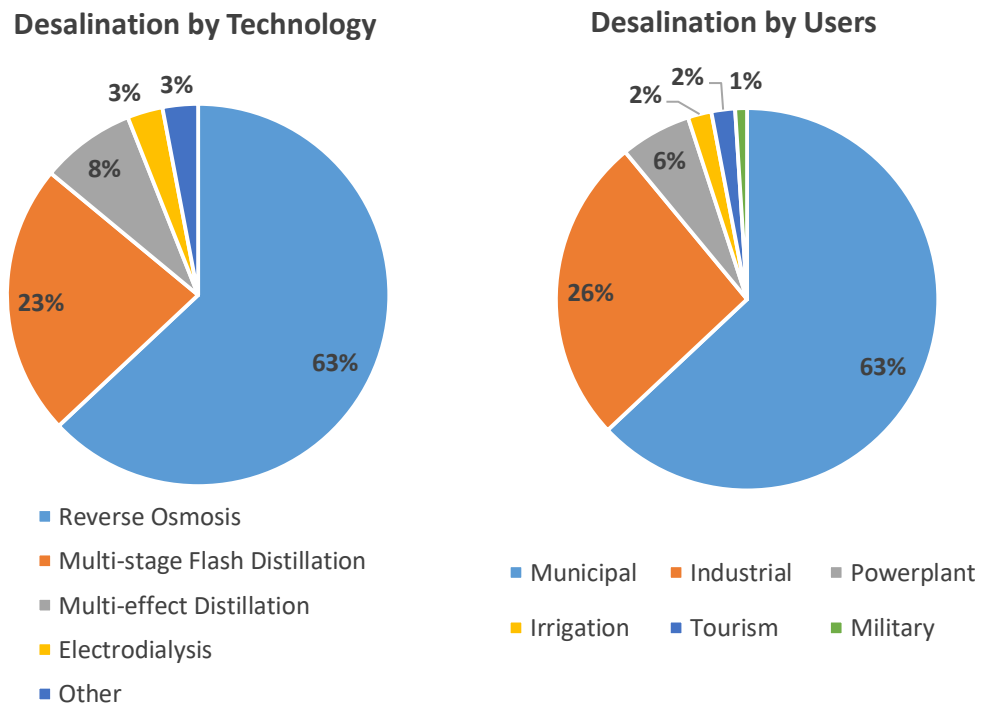


**Figure 1.2** Global desalination industry share by technology and users [5].

The worldwide desalination capacity is increasing at a steadfast pace depending on the rising demand for freshwater and developing technologies. In 2007, the total global desalination capacity was 47.6 million m<sup>3</sup>/d, in 2008 it rose 58 million m<sup>3</sup>/d, in 2011 it reached to 65.2 million m<sup>3</sup>/d and then to 74.8 million m<sup>3</sup>/d in 2012 [5, 28]. The International Desalination Association (IDA) reported that in 2015, there were 18,426 desalination plants installed worldwide with a treating capacity of 86.8 million m<sup>3</sup> of water per day. These plants serve fresh water to more than 300 million people in 150 countries [29].

Even though membrane and thermal desalination technologies provide effective deionization, the major limitations of these conventional deionization technologies are high energy requirement and secondary pollutant generation; therefore, significant operational/maintenance cost of these processes. Conventional desalination technologies use high-pressure membranes and high temperatures to provide effective ion removal from water. Most of the existing industrial scale desalination facilities obtain their energy from the combustion of fossil fuels, thus this exchange of CO<sub>2</sub> emissions for freshwater production enhances global warming and eventually contributes to the depletion of freshwater resources. Also, these processes add treatment chemicals into water that have harmful effects on the environment and living organisms [17, 29 - 33]. Because of these reasons, developing more energy efficient, economical and environment-friendly methods for sea/brackish water desalination has become highly crucial.

Capacitive deionization (CDI) technology is a novel alternative water treatment process that can be effectively used for desalination. This electrochemical deionization method uses supercapacitor electrode technology to remove ions from water in a more economical and environmental way. Compared to other deionization processes, CDI technology has become more attractive to researchers in recent years with the developments in nanomaterials technology and its high potential to replace today's desalination technologies [7, 13, 17].

### **1.3. Motivation and Aim of the Study**

Considering the global challenge of water supply and the disadvantages of conventional desalination technologies, it is necessary to explore, improve and implement new technologies to overcome water scarcity in a more energy and cost efficient, and environmental-friendly way. CDI process, as an electrochemical desalination tool, is the first developed desalination technology in more than 50 years [30], and is considered as a very promising and effective ion removal technology in the desalination field. CDI technology has high potential to be an energy efficient desalination method; therefore, it is important to improve and adapt this technology to real life applications.

The overall aim of this thesis is the investigation of ion removal performance of the CDI process under various operating conditions.

The specific objectives of this study are;

1. To investigate the effect of different operational parameters (applied voltage and water flow rate) on electrosorptive capacity of the CDI process,
2. To investigate the selective ion removal behavior of carbon based electrodes having different structural properties using monovalent and divalent ions at varying concentrations,
3. To compare the ion removal efficiencies of two different electrode materials: activated carbon and graphene,
4. To investigate the regeneration behavior and long term use of the CDI process.



## CHAPTER 2

### LITERATURE REVIEW

#### 2.1. Capacitive Deionization Technology

Capacitive deionization (CDI) technology is a novel, electrochemically controlled sorption/desorption process that promotes the removal of charged ionic species like; salt ions, hardness, heavy metals, arsenic etc. from different types of water [30, 34]. In CDI process, the feed water is passed through a cell consisting of electrode couples made of conductive porous materials while direct current is applied to the cell. In this electrosorption step, ions in the feed water are held onto the charged electrode surfaces, resulting in the removal of ions from water. After a period of time, the electrodes become saturated, then the applied voltage is removed or reversed in order to release the ions back into the concentrate flow and achieve regeneration of the electrodes [17, 35]. These electrosorption (charge) and desorption (discharge) steps can be alternated to produce purified water and concentrated brine, respectively. Schematic description of the CDI process is given in Figure 2.1.

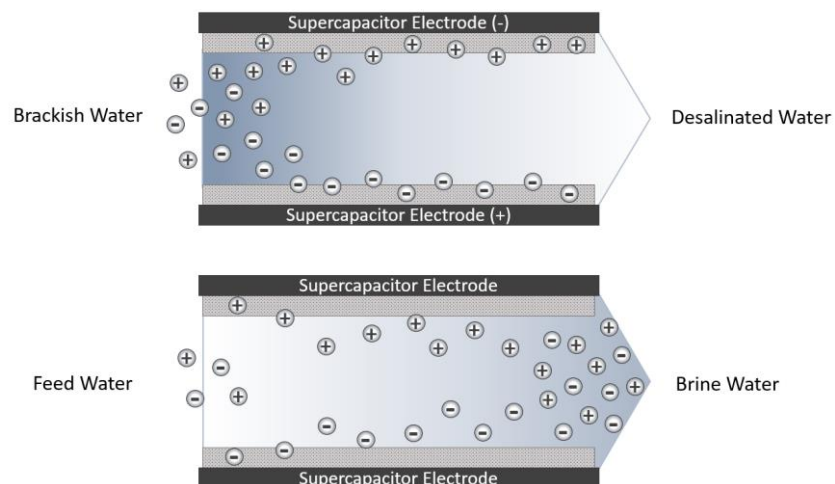
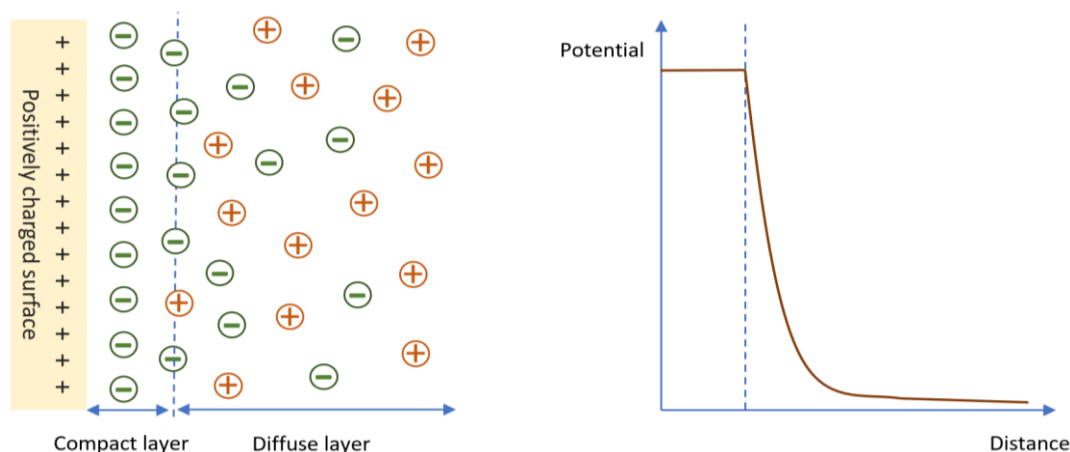


Figure 2.1 Schematic description of the CDI process.

## 2.2. Working Principles of the CDI Process

There are two fundamental mechanisms employed for ion storage in the CDI process. The main mechanism is based on the electrical double layer (EDL) formation. When electric potential is applied to the electrodes, anions and cations in the solution are attracted to and adsorbed onto the charged counter electrode surface (with an opposite charge to that of the ion) with the help of electrostatic forces (Coulomb force), forming EDL. Removing the potential hence the electrostatic forces releases the ions back to the solution. This taking up and release mechanism is used as deionization and regeneration operation in the CDI process [36 - 38]. Simplified schematics of the EDL mechanism is as shown in Figure 2.2. Interfacial properties and structure between an electrode and an aqueous solution is explained well by Gouy-Chapman-Stern double layer theory. According to this theory, the EDL is assumed to be divided into two different regions, which are *compact* layer (Helmholtz layer), where ions directly cover the surface of the electrode, and a *diffuse* layer (Gouy–Chapman layer), where the distribution of electric charge depends on the potential at the surface. Capacitance of both of the inner layer and diffuse layer contribute to the total capacitance of the system [39, 40]. This mechanism is dependent on electrostatic charge accumulation at the surface of the materials like carbons and their derivatives [38].



**Figure 2.2** Representation of the electrical double layer and potential distribution.

Another mechanism that can take place during CDI operation is Faradaic charge transfer (pseudocapacitance). While in EDL mechanism ions are only stored physically on the surface of the carbon based electrodes, Faradaic ion storage processes result in an electron transfer between ions and pseudocapacitive electrode materials through fast, reversible electrochemical reduction/oxidation reactions at the electrode and solution interface. Therefore, it causes another adsorption/desorption like mechanism that makes it possible to hold on more ions on the electrode surface. Some of the most commonly investigated pseudocapacitive electrode materials are metal oxides for the capture of cations and conductive polymers for the bonding of anions [41, 42].

### **2.3. Historical Development and Current Status of the CDI Technology**

The concept of CDI technology was first introduced in the mid-1960s by Caudle group based on flow-by system in which saline water was pumped through the charged electrode sheets. Then in early 1970s the process was improved by Johnson group as a reversible electrosorption model that allows regeneration of the electrodes by removing the electrical field, which defines the fundamental concept of the CDI process [39, 42]. Studies on CDI were eventually discontinued mainly because of the instability of electrodes (especially the anode); however, preliminary evaluations about the CDI technology showed that efficient, low-cost desalination can be achieved provided that sufficiently stable, high-surface area electrodes are produced [7, 40].

Over the last twenty years however, researches described the process with physical theories and disclosed breakthroughs in electrode materials and preparation, cell configurations and operational modes. This have generated renewed interest in the CDI technology from both water treatment and energy recovery perspectives [39, 42]. Thus, the number of studies in the CDI field increased enormously since year 2000 (Figure 2.3).

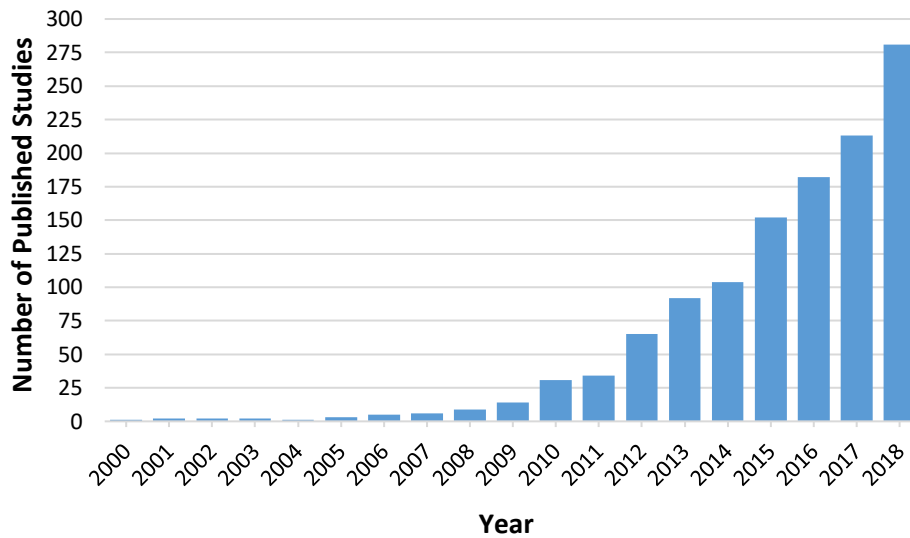


**Figure 2.3** The number of studies published in the CDI field since the year 2000 [43].

Despite the significant number of studies related to CDI technology that are ongoing for more than fifty years, the pilot scale applications of the CDI process are quite limited [30, 40]. To our knowledge, there have been only four laboratory studies carried out using a pilot scale CDI unit with the highest flow rate at 3,785 m<sup>3</sup>/day. These studies were performed in order to examine the effect of temperature and other operational parameters on the efficiency of the CDI process using synthetic water [8]. In addition, some pilot scale studies were also conducted to investigate CDI process application in real world conditions. In 2013, a portable prototype CDI unit was used for inland brackish groundwater desalination in a remote location of Australia [44]. The water flow rate was around 10,000 m<sup>3</sup>/day and the total water recovery rate of the process was between 75% and 80% in this research. The system was able to remove Ca<sup>2+</sup>, Mg<sup>2+</sup> and Na<sup>+</sup> ions along with other inorganic compounds. Same group conducted another pilot scale study again in Australia [45] in order to investigate TDS removal from lakes. As a result of this study, it is found that TDS removal efficiency of the CDI electrodes decreased with time, possibly due to fouling problem, which was attributed to high organic content present in the lakes.

In general, these pilot scale studies provided a good base of knowledge about the CDI process and defined several factors that need to be optimized and developed to take the CDI technology to industrial level. However, more studies are needed for greater understanding of the issues related to the process under various conditions and using different electrodes prior to the successful transition of the CDI technology from laboratory to large scale water treatment plants. Also, a stronger understanding of design and operation of CDI systems is essential in order to optimize the process performance and to improve its stability over time [8, 37]. These issues are important for CDI technology to close the gap between research and practice; especially for complying with real-life conditions including different water qualities and determining possible applications of the CDI process.

#### **2.4. Advantages and Limitations of the CDI Process**

CDI technology offers significant advantages that overcome economic and environmental problems related to conventional deionization technologies. The most important advantage of CDI process is its high energy efficiency. CDI technology consumes low energy since it does not require any high pressures or temperatures, unlike membrane and thermal based deionization processes, and works under very low voltages (1.2 - 2 V) [17, 35]. Another reason for CDI being an energy efficient technology is that it does not need any energy transformation from other energy sources - it can directly use electrical energy avoiding the energy losses that might occur during energy conversion processes.

Since the CDI technology uses energy storing electrodes to deionize water, it is possible to recover a part of the energy used. In the regeneration step while ions are released from the surface of the electrodes, some of the applied energy is released as well. This energy can be stored with the help of supercapacitor electrodes and used to charge another CDI unit that works in parallel. As a result, energy used in the CDI system can be recovered by 50 - 70% [30, 34, 35]. It is shown that especially for typical brackish water treatment, CDI process needs less energy to deionize water (0.6

kWh/m<sup>3</sup>), as compared to EDR (2.04 kWh/m<sup>3</sup>) and RO (2.25 kWh/m<sup>3</sup>) processes, which are considered as the most efficient desalination techniques presently available [30, 46].

Moreover, CDI process can reach higher water recovery rates (ratio of the volume of desalinated water to inlet water) up to 90% [47] as compared to conventional membrane deionization processes, which has a recovery rate less than 75% for brackish water treatment and less than 45% for seawater desalination, where scaling fouling is the main challenge in exceeding these rates. Water recovery rates are even lower for the thermal desalination technologies [48, 49]. Although high water recovery rate is advantageous for CDI process, since it ensures reduction in brine volume, it may cause disposal problems as the water recovery increases, the salt concentration in the brine stream also increases [47, 50].

Furthermore, conventional deionization processes need lots of maintenance, like continuous use of chemicals in the system such as chlorine species (NaOCl, FeCl<sub>3</sub>, AlCl<sub>3</sub>) and acids (H<sub>2</sub>SO<sub>4</sub>, HCl, C<sub>6</sub>H<sub>8</sub>O<sub>7</sub>) in order to prevent scaling and membrane fouling problems, which are then discharged to the environment as a secondary pollutant in a waste brine stream that can cause serious environmental problems. These chemicals require a further treatment prior to safe discharge to the environment [7, 12, 13, 17]. In addition, high temperatures are used in thermal deionization processes to desalinate water that then rises the temperature of brine stream causing thermal pollution and disposal problems. Increased temperatures reduce oxygen solubility in water and significant decrease in the oxygen levels can be toxic for aquatic environments and lethal to immobile and unadjusted organisms [12]. On the other hand, since CDI process do not require any membrane or heating system; it requires less maintenance and creates less environmental and disposal concerns compared to conventional deionization processes. Thus, CDI technology can easily be designed as a package or decentralized treatment system [36].

In addition, for brackish water treatment, it was estimated that the cost of CDI technology may be much lower compared to conventional treatment processes, including capital, operation and maintenance costs. Capital cost constitutes more than half of the total cost of the CDI system [30]. Only by reducing the costs for the CDI units, particularly by producing cheaper/more effective nanomaterials, CDI technology would become a serious competitor for conventional deionization processes in high salinity brackish or seawater applications.

## **2.5. Materials Used in CDI Electrodes**

### **2.5.1. Electrode Active Materials**

Electrode materials are considered as the most important components in CDI devices, since they play a significant role in the electrosorption process. With the recent advancements in material science, nanostructured materials with superior features have started to be widely used to develop advanced supercapacitor electrodes. By using these improved materials, it is possible to increase the active surface area of the electrodes; thus, the higher process efficiencies can be achieved [51]. In recent years, this field is combined with the rapidly growing knowledge of the CDI technology in order to increase the ion removal efficiency from water.

Electrode materials used in the supercapacitor electrodes of CDI process should have some specific properties for efficient ion removal. Since ions are stored at the electrode/solution interface; briefly, ideal electrode materials are considered to have a large ion-accessible specific surface area and suitable pore size to accumulate considerable amount of ions without diffusional and kinetic limitations. In addition, high conductivities are required for decreasing the contact resistance between the electrode and the current collector to avoid energy dissipation and voltage drop between them [7, 39, 52]. Also, they should have good wetting behavior (hydrophilicity), which ensures that the entire pore volume is participating in the CDI process. Furthermore, they should have high electrochemical stability over the used

pH and voltage range, as well as high bio-inertness to prevent biofouling problem to provide system durability for long-term operation [7, 53].

Moreover, the ideal electrode materials for large-scale applications should have high natural abundance, scalability and low carbon footprint. Availability and environmental impacts not only affect the cost considerations, but also the sustainability concerns. Also, they should be processable and shapeable into film electrodes [7, 40].

Carbon-based materials, metal oxides and conducting polymers are widely used electrode materials for CDI devices [37, 39]. It is possible to produce supercapacitor electrodes using either of those materials separately or together as nanocomposite supercapacitor electrodes. Timeline of the most commonly used electrode materials in CDI applications is provided in Figure 2.4.

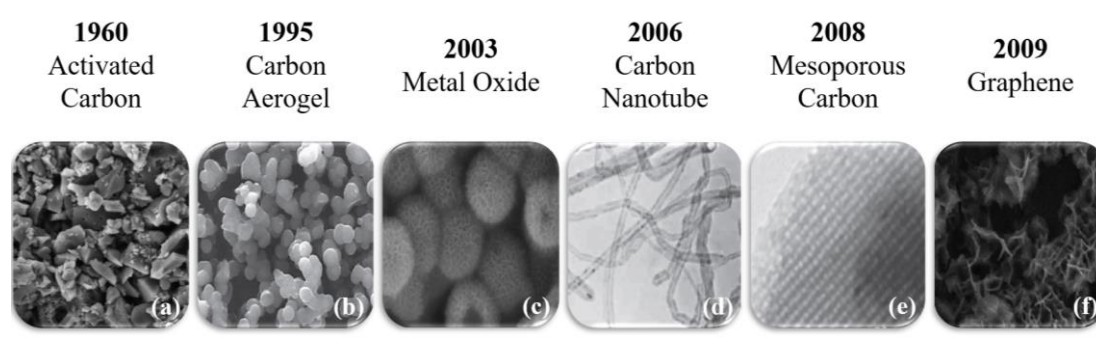


**Figure 2.4** Timeline of the materials used in CDI electrodes: (a) activated carbon [54], (b) carbon aerogel [7], (c) metal oxide [55], (d) carbon nanotube [7], (e) mesoporous carbon [7], (f) graphene [56].

### 2.5.1.1. Carbon Materials

Carbon materials are widely used in supercapacitor electrodes because of their highly desirable properties. They typically have high specific surface area, good conductivity, controllable porous structure and good processability. Ion storage mechanism of carbon materials is based on holding the ions in the form of EDL on the electrode/solution interface. Carbon based electrodes show low contact resistance

(voltage drop from electrode to the current collector), appropriate wetting behavior and chemical stability. Therefore, they generally show good electrosorption performance in the CDI process. Carbon-based nanomaterials such as activated carbon (AC), carbon aerogel (CA), carbon nanotube (CNT), ordered mesoporous carbon (OMC) and graphene (GR) are widely used electrode materials for the CDI process [17, 37, 44, 51].

#### Activated Carbon:

Among carbon materials, AC stand out as the first electrode material used in CDI systems. ACs are the most abundant carbons that can be derived from carbon-rich natural sources such as wood, coconut shells, coal or synthetic sources like resins through carbonization in inert atmosphere. The combination of a low cost (50 \$/kg) and a high specific surface area (1000 - 2000 m<sup>2</sup>/g) makes these materials particularly attractive for many water separation and purification applications including the CDI process [7, 39, 53, 57].

AC is the most commonly investigated electrode material in CDI applications, due to its easy fabrication and low cost [39], especially considering large scale applications. However, pure AC based electrodes had quite low electrosorptive capacity due to their irregular pore structure and low conductivity. Therefore, studies using AC based electrodes were mainly focused on improving their structural properties and wetting behavior using different chemical treatment methods. Related studies aimed at introducing hydrophilic surface groups to the hydrophobic AC by potassium hydroxide (KOH) [22, 58] and nitric acid (HNO<sub>3</sub>) [58, 59] as activating agents. It was found that, although the surface area and average pore size of the materials remain the same following the treatment, it is possible to reach higher electrosorptive capacities due to more hydrophilic nature of the material, resulting in improved wetting. Also, it has been found that some materials, such as some metal oxides and GR, can be used in conjunction to AC to produce nanocomposite electrodes and improve the capacitance of the CDI electrodes [7, 39, 53].

### Graphene:

GR is a two-dimensional single-atom layer structure carbon material, which can be produced through chemical vapor deposition (CVD) or exfoliation methods. GR has attracted a lot of interest as an electrode material in the CDI process recently, since it shows promising properties, such as large surface area, high electrical conductivity ( $\sim 2000$  S/cm) and chemically stable electrochemical storage capacity. Also the open interlayered structure of GR sheets provides a short path and access for ions to diffuse to the electrode; hence, leading to easy electrosorption and desorption in the CDI processes [31, 39, 53, 60, 61].

The first research on the electrosorption performance of GR-like electrodes for CDI has shown that the ion removal performance of GR is higher than AC. However, it has been observed that two dimensional structure of GR causes aggregation and decrease in the electrode surface area as well as its ion adsorption capacity [56]. Therefore, several researchers have focused on the synthesis of three dimensional (3D) GR structures to prevent this drawback. Their results have shown that 3D GR structures show higher capacitance, higher specific area, larger pore volume and better electrosorption performance in CDI application compared to two dimensional GR. This was attributed to the easy movement of ions in the 3D electrodes [62, 63]. In addition, it was demonstrated that 3D GR based electrodes are also promising for the separation and recovery of heavy metals and salt ions from the wastewater [64]. In addition to pure GR based electrodes, there are studies using GR composite electrodes with other carbonaceous or metal oxide materials [37, 39, 53].

### Carbon Aerogel:

CA have a 3D, nanosized air-filled foam structure and used as another electrode material especially in the earliest CDI cell designs. Generally, CAs are synthesized using a sol-gel process, by transforming precursors like resorcinol-formaldehyde into a highly porous network [39, 65]. Due to their structural strength, good electrical conductivity (10 - 100 S/cm), moderate specific surface area (400 - 1000 m<sup>2</sup>/g) and

mesoporous pore size CAs are considered as suitable electrode materials for CDI applications. However, fouling of aerogel surface by natural organic matter prevents their use for the effective treatment of natural water [7, 39, 53].

#### Ordered Mesoporous Carbon:

Another carbon material used in CDI electrodes is OMCs, which are produced by either the hard-template or the soft-template methods. Unlike most ACs with microporous structure, OMCs have periodic arrangements of mesopores in the range of 2 - 50 nm, which can improve the ion transport through the pore network. This arrangement makes the specific surface area of OMCs (750 - 1500 m<sup>2</sup>/g) comparable to many ACs. However, the synthesis and preparation of these materials can be costly and time-consuming, and are impractical for most of the CDI systems [7, 39].

#### Carbon Nanotube:

CNTs are cylindrical shaped carbon forms, typically produced through CVD method. These materials are mostly composed of mesopores and considered as good electrode materials for CDI process, because they possess high conductivity and chemical stability. Their surface area (120 - 500 m<sup>2</sup>/g) can be considered as low compared to other carbonaceous materials. However, almost all the area is ion accessible which makes CNTs favourable for the CDI applications. In contrast, their hydrophobic nature and tendency to agglomerate may block access to the surface adsorption sites and decrease the ion removal efficiency. Among CNTs, single walled carbon nanotube (SWCNT) and multi-walled carbon nanotube (MWCNT) based electrodes and their composites perform well for water treatment. Yet, they are not economically feasible for large scale applications [7, 39, 44, 66].

### 2.5.1.2. Metal Oxides

Metal oxides are also used as supercapacitor electrode materials because of their pseudocapacitive feature. Their ion storage mechanism is based on the Faradaic reduction/oxidation reactions including anodic oxidation, cathodic reduction and Faradaic ion storage processes occurring on the surface of and within the electrode materials [53]. Although, most of the metal oxides have poor conductivity, they typically have high theoretical capacitance, low cost, environmentally benign nature, natural abundance and they can be easily anchored onto the carbon structure, which makes them a good alternative electrode material for the CDI applications. Metal oxides possess several advantages on top of carbon materials and can enhance capacitive behaviours and adsorption efficiency of the CDI process. Especially AC, CNT and GR are considered as promising conductive base materials for metal oxides in CDI electrodes [67 - 71].

Many metal oxide/carbon composite electrodes were studied in CDI applications. Among metal oxides, titanium dioxide ( $\text{TiO}_2$ ), manganese oxide ( $\text{MnO}_2$ ), zinc oxide ( $\text{ZnO}$ ) and tin oxide ( $\text{SnO}_2$ ) are the widely used in CDI electrodes [69, 72 - 74]. In general, these composite materials present good electrochemical performance with low polarization resistance, fast electrosorption ability and high hydrophilicity. However, it has been observed that some metal oxides like  $\text{ZnO}$  release additional ions into the water during the operation, which may affect the conductivity of solution and is not suitable for CDI applications. Also, the introduction of some metal oxides like  $\text{TiO}_2$  onto the surface of carbon-based materials led to a decrease in the specific surface area of electrodes attributing to  $\text{TiO}_2$  blocking some of the surface pores of the carbon-based materials. As a result, physical adsorption capacity of CDI electrodes decreases [53, 75].

### 2.5.1.3. Conducting Polymers

Conducting polymers are another class of pseudocapacitive materials used in supercapacitor electrodes. Ion storage mechanism of conducting polymers is similar to metal oxides and is based on Faradaic reduction/oxidation reactions. They typically have high specific capacitance values, high conductivity when doped, easy fabrication and low cost, making them suitable as electrode materials. Conducting polymers are commonly incorporated with different carbonaceous materials such as AC, CNT and GR or metal oxides like  $\text{MnO}_2$  for CDI applications. Conducting polymer-carbon composite electrodes can enhance the adsorption capacity in a CDI cell as well as the conductivity of the electrode material. Thus, there is no need for conductive additives for such electrodes [53, 76].

Polyaniline (PANI) and polypyrrole (PPy) are two common conductive polymers which have been extensively studied as electrode materials for the CDI process [77, 78]. In general, PANI exhibits higher mechanical strength and capacitance as compared to PPy, whereas PPy displays higher electrical conductivity and much stable electrochemical properties at a wide range of pH, which is limited to acidic pH for PANI. Also, since PANI has a toxic nature, its widespread application for water reclamation and reuse is limited. There are studies in which the performance of these materials in the CDI setup were investigated individually and combined [39, 53, 79].

An overview of various studies on the use of carbon materials including their metal oxide and conducting polymer composites as electrode materials for CDI applications is provided in Table 2.1 with their ion removal performances.

**Table 2.1** Electrosorption capacities of different electrodes used in CDI applications.

Electrode Material	Experimental Conditions			Electrosorption Capacity	Ref.
	Initial NaCl Concentration	Flow Rate	Cell Voltage (V)		
<b>Carbon Materials</b>					
AC	25 mg/l	14 ml/min	1.2	4.3 $\mu\text{mol/g}$	[80]
	50 mg/l	7.2 ml/min	1.2	761.46 $\mu\text{mol/g}$	[81]
	100 mg/l	20 ml/min	1.2	104.38 $\mu\text{mol/g}$	[82]
	200 mg/l	30 ml/min	1.5	62.97 $\mu\text{mol/g}$	[83]
CA	50 mg/l	400 ml/min	1.7	22.25 $\mu\text{mol/g}$	[84]
	50 mg/l	25 ml/min	1.2	23.96 $\mu\text{mol/g}$	[85]
	500 mg/l	25 ml/min	1.2	49.62 $\mu\text{mol/g}$	[85]
CNT	23 mg/l	25 ml/min	2.0	12.79 $\mu\text{mol/g}$	[66]
	60 mg/l	-	1.2	73.58 $\mu\text{mol/g}$	[86]
	60 mg/l	6 ml/min	1.2	22.25 $\mu\text{mol/g}$	[87]
OMC	25 mg/l	14 ml/min	1.2	11.6 $\mu\text{mol/g}$	[80]
	50 mg/l	20 ml/min	0.8	15.9 $\mu\text{mol/g}$	[88]
GR	25 mg/l	25 ml/min	2.0	23.18 $\mu\text{mol/g}$	[3]
	25 mg/l	40 ml/min	2.0	31.66 $\mu\text{mol/g}$	[56]
	50 mg/l	25 ml/min	1.6	49.62 $\mu\text{mol/g}$	[62]
	65 mg/l	20 ml/min	2.0	56.47 $\mu\text{mol/g}$	[9]
<b>Carbon Composites</b>					
AC / GR	500 mg/l	25 ml/min	1.2	50.31 $\mu\text{mol/g}$	[89]
CNT / GR	25 mg/l	25 ml/min	2.0	24.13 $\mu\text{mol/g}$	[90]
OMC / CNT	40 mg/l	25 ml/min	1.2	11.81 $\mu\text{mol/g}$	[91]
OMC / GR	30 mg/l	25 ml/min	1.6	39.36 $\mu\text{mol/g}$	[92]
<b>Metal Oxide Composites</b>					
MnO <sub>2</sub> / AC	25 mg/l	20 ml/min	1.2	16.3 $\mu\text{mol/g}$	[69]
MnO <sub>2</sub> / GR	50 mg/l	-	1.2	85.56 $\mu\text{mol/g}$	[25]
TiO <sub>2</sub> / AC	100 mg/l	12 ml/min	1.2	137.75 $\mu\text{mol/g}$	[93]
TiO <sub>2</sub> / CNT	500 mg/l	80 ml/min	1.2	73.58 $\mu\text{mol/g}$	[67]
SnO <sub>2</sub> /GR	30 mg/l	-	1.4	25.50 $\mu\text{mol/g}$	[73]
ZnO / AC Cloth	100 mg/l	2 ml/min	1.2	145.45 $\mu\text{mol/g}$	[33]
<b>Polymer Composites</b>					
PANI / AC	250 mg/l	-	1.2	53.90 $\mu\text{mol/g}$	[77]
PANI / SWCNT	50 mg/l	20 ml/min	1.2	-	[94]
PPy / GR / MnO <sub>2</sub>	500 mg/l	10 ml/min	2	314.85 $\mu\text{mol/g}$	[79]

### **2.5.2. Conductive Additives**

Conductive materials like carbon black and graphite are usually added into CDI electrodes, in order to improve the electrical conductivity of the electrodes. It has been shown that the main feature of conductive additives that affects the CDI process efficiency is their pore structure. Conductive additives with a high fraction of mesopores can significantly increase the specific capacitance of the electrodes [95]. Generally, conductive additive amounts used in CDI electrodes are changing between 5 - 10 wt.% for carbon black [67, 96, 97] and 5 - 20 wt. % for graphite [69, 78, 93].

### **2.5.3. Polymer Binders**

Polymer binders are used in the CDI electrodes to provide structural stability and to fix them onto the current collector. The most commonly used binders in CDI electrodes are polytetrafluoroethylene (PTFE) and polyvinylidene fluoride (PVDF). Using large amounts of these hydrophobic binders may decrease the surface area of the electrodes by blocking access to the pores and reduce their wettability [98]. Thus, it is important to use them in a minimum amount that provides enough mechanical strength to the electrodes, which is usually changing between 5 - 20 wt. % for PTFE [9, 67, 99, 100] and 5 - 13 wt. % for PVDF [39, 54, 55] in CDI applications.

### **2.5.4. Current Collectors**

The current collector is an electrically conductive material used to transmit applied voltage and provide an attachment surface for CDI electrodes. Briefly, the proper current collector material should be resistant to corrosion and electrochemically stable in the applied working voltage range of the CDI system. Thus, graphite materials in a form of sheet or paper are used as a current collector for most of the CDI electrodes [9, 74, 101]. Other current collectors used in CDI electrodes include carbon fiber paper/sheet [102, 103], stainless steel foil [104, 105], nickel foam [106] and titanium foil [93, 107].

## 2.6. CDI Process Configurations

### 2.6.1. Unit Cell Geometries

CDI modules can be designed in different geometries and be used as a single cell or a stack unit combining multiple cells [35]. Generally, symmetrical electrode systems are used in CDI configurations, where the anode and cathode electrode masses are equal; however, there are several studies which used asymmetric electrode geometries with different anode and cathode mass ratios for the separation of ions from water [3, 96].

In the majority of experimental studies on CDI process, units were designed as flow-by mode (Figure 2.5 (a)), in which the electrodes with a thickness of 100 - 500  $\mu\text{m}$  are arranged parallel to each other and water is passed through the small gap between those electrodes. The open channel between the electrodes can be designed as typically at least 1 mm thick. Alternatively, a porous spacer film with thickness between 100 and 300  $\mu\text{m}$  can also be used for this purpose [7, 53]. Generally, instead of a one-dimensional water flow, water is passed through one edge of a channel and directed to an outlet point at the opposite corner. In this case, it is aimed to hold more ions on the surface of the electrodes by increasing the retention time of the water in the cell. Typical electrode areas used in this classical CDI geometry in laboratory scale experiments varies from 5 x 5  $\text{cm}^2$  to 10 x 10  $\text{cm}^2$  [7].

As an alternative to classical CDI geometry, flow-through mode was developed by Suss et al. [108], in which the electrodes were placed perpendicular to the running water (Figure 2.5 (b)). In this design, the inlet water is pumped straight through the pores in the electrodes, which allows process to take place faster than conventional geometry since ions can directly migrate to the electrodes without diffusing from the spacer channel.

Another approach is so-called electrostatic ion pumping (Figure 2.5 (c)), where purified water and concentrated brine stream emerge from different points semi-

continuously. In this method, water is being fed continuously through the inlet hole and during electrosorption and regeneration steps effluent water is directed to different exit channels of the CDI cell using valves. Hence, two separate freshwater and brine streams are produced [109].

Alternative design employs movable carbon rod electrode wires (Figure 2.5 (d)). In this design after the electrosorption step where salt ions are adsorbed into the electrodes, the wire pairs are moved into another water stream for regeneration step to release ions. Thus, the freshwater and concentrate streams are produced continuously and separated at all times, unlike other configurations where the freshwater and brine are produced from the same device at different periods of time [110].

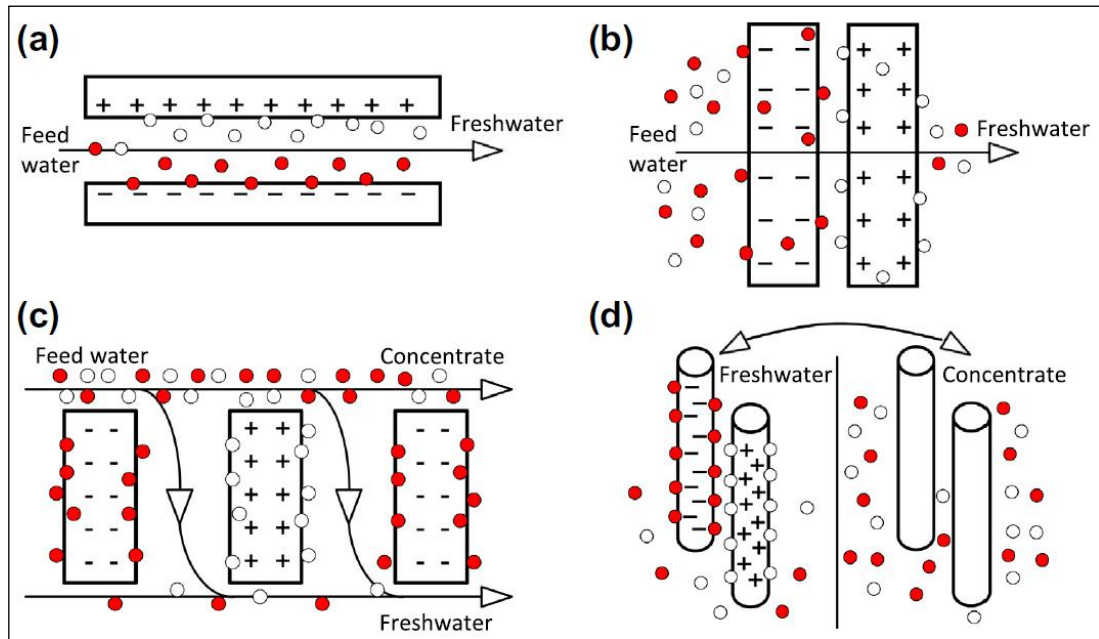


**Figure 2.5** The most widely used CDI system configurations; (a) Flow-by mode, (b) Flow-through mode, (c) Electrostatic ion pumping and (d) Deionization using wire electrodes [7].

### 2.6.2. Process Operating Systems

Other than the electrode materials and system geometries, the operating conditions of the CDI process also have a significant importance in the system performance. Mainly, CDI systems are operated in two ways namely; single-pass or batch mode. In

single pass operation, saline water is pumped from a tank into the CDI cell and then effluent is collected in another tank. Salinity measurements are done before and after the water passing through the CDI unit. Single pass treatment systems may face with various operation problems, like change in ion concentration of the solution over the time. At the beginning, the ion concentration is close to the inlet water, while it decreases significantly over time to reach the treated water level. In parallel with the ion concentration, physicochemical properties (pH, conductivity, viscosity, density) of the water also change. These changes may require continual adjustments in water flow rate, current and voltage to ensure constant ion removal, which makes it difficult to determine fixed operating parameters [7, 35]. Recycle modification is designed to overcome the difficulties observed at the single pass operating system. In these modified systems, a certain amount of the effluent water is recycled to the CDI units by mixing with the influent water. Thus, it is possible to adjust the concentration difference between the inlet and outlet water by changing the recycling rate. At high recycled water / inlet water ratios, the ion concentration in the system will remain almost constant, so does the physicochemical parameters, providing easier operation for especially the real-life conditions, where continuous water treatment is required. However, single pass operation systems can be impractical for research and laboratory studies especially for long term experiments, since larger quantities of water are required [7, 111].

On the other hand, batch mode operation systems constitute the most frequently studied and reported CDI experimental setup. In this configuration, a fixed volume of saline water is pumped from a tank into the CDI unit and effluent water is collected back in the same tank. The water is recycled in the CDI unit during the experiments and this process generally continues until the water salinity becomes constant. The salinity measurements are made either in the tank or by using inline measurement probes [7].

## **2.7. CDI Process Operation Parameters**

### **2.7.1. Applied Voltage**

Applied voltage is one of the most important operational parameters in CDI process, since it acts as the main driving force for ion adsorption and significantly affects electrosorptive capacity and electrosorption rate in CDI systems. Generally, it is predicted that applying higher voltages to the electrodes increases the electrosorptive capacity, as it enhances charge and electrostatic forces at the electrode-solution interface based on the EDL theory and decreases the system resistance. However, increasing the electrical potential above a certain limit may lead to electrolysis of water and reduction in electrosorption performance of a CDI unit [53, 82, 112]. Thus optimum operation voltage should be determined in order to achieve the highest ion removal.

The effect of applied potential on the ion removal performance of CDI process have been investigated in many studies. In general, previous studies reported that there is a positive relationship between the applied voltage and ion removal rates as expected. While increasing the applied voltage, ion adsorption capacity of a CDI system increases exponentially to a point and continues to increase slightly until it reaches the optimum operation voltage, and then starts to decrease mainly because of the increased parasitic effects of the water electrolysis [31, 53, 112]. Different optimum operation voltages such as 1.2 V [113], 1.57 V [114], 1.8 V [115] and 2.0 V [31] were reported in the literature where the CDI system reaches its highest electrosorption capacity with carbon based electrodes. These results indicate that optimum applied voltage for CDI operation is highly dependent on the system design and electrode properties. Although the theoretical potential needed for the water electrolysis is 1.23 V, it was not observed even at higher potentials in most of the experiments due to the presence of large resistance in the circuit systems [53]. Despite the fact that optimum applied voltage of a CDI system is highly dependent on the unit configuration, system

charge efficiency and electrode materials, an applied voltage of 1.0 – 2.0 V is considered as appropriate for most of CDI applications.

### **2.7.2. Flow Rate**

Water flow rate is considered as having a direct relationship with ion adsorption capacity in a CDI system. Especially in single pass experimental setups, flow rate plays a critical role in determining the time period that the salt can interact with the electrodes. In addition, it is expected to achieve higher ion removal efficiencies at slower flow rates, since the feed solution interacts longer with the electrodes [116, 117]. On the other hand, in batch mode experimental setups flow rate has a less significant effect since the same volume of water is in contact with the electrodes. This affects several important parameters such as mixing of the water in the CDI cell and the recycling tank [118].

As a result of the previous studies using batch mode experimental setups, it has been found that ion adsorption capacity of a CDI unit increases with the flow rate up to a certain point and then starts to decrease significantly. This signifies that there is an optimal flow rate. This is probably because flow rates that are too low result in a co-ions effect that suppresses the electrosorption process, while flow rates too high create stronger pumping force higher than electrosorptive force and therefore decreases the electrosorption capacity of the electrodes. Therefore, equilibrium between the electrostatic force and the driving force should be maintained in order to achieve optimum flow rate for a CDI system [31]. Previous studies defined different optimum flow rates for batch mode experimental setups. However, these values are inapplicable to other CDI systems because of their differences in size, scale and design [118]. Yet in general, flow rates up to 25 ml/min is widely accepted as proper values for most of the batch mode CDI experimental setups.

### 2.7.3. Initial Salt Concentration and Ion Type

Initial salt concentration in the feed water is another important parameter affecting the CDI process performance. Thus, it is important to understand the electrosorptive behavior of a CDI system based on the salt concentration, especially for relating ion removal from water with various characteristics. Since CDI technology is primarily considered as a brackish water treatment process, related studies usually conducted using synthetic sodium chloride (NaCl) solutions with a concentration below 3,000 ppm as feed water. As a result of these studies, it has been shown that the ion adsorption capacity of a CDI system increases as the salt concentration in influent water rises, as predicted from EDL theory. In addition, it has been found that higher influent salt concentration has a positive effect on certain desalination metrics, such as electrosorption mechanism and energy consumption, mainly because of the greater conductivity of the water [118].

The type of the ionic species is also an important parameter especially considering the selective ion removal. Valence number and hydrated radius of the ions are the main characteristics that affects their electrosorption behaviour. In most of the related studies, monovalent ( $\text{Na}^+$ ) and divalent ( $\text{Ca}^{2+}$ ,  $\text{Mg}^{2+}$ ) ions were investigated. Ions with higher valence have stronger electrostatic interactions, and therefore they are expected to have higher electrosorption ratio compared to monovalent ions. However, previous studies have shown two contrary results on the removal of different ion species. It was reported that monovalent ions are preferentially removed than divalent ions [119], while different results were obtained by several researchers [31, 120, 121], which indicates that using electrodes with different structural properties significantly effects electrosorption efficiency of different ions and would result in the opposite trends in ion removal.



## CHAPTER 3

### MATERIALS AND METHODS

#### 3.1. Preparation of the Lab-scale CDI Unit

The laboratory scale CDI unit used in the experiments was designed as two parallel electrode configuration system. A photograph of the manufactured CDI unit used in the experiments is provided in Figure 3.1. The cell is manufactured from two 20 cm x 20 cm size and 1 cm thick plexiglass units, including a water channel between them with a 1 - 1.5 mm opening. An elastic ring (O-ring) is inserted around the water channel to provide system water impermeability. Plexiglass units are attached to each other using screws with plastic rings around them, which makes it easy to open the CDI unit and replace the electrodes. Plexiglass material prevents the cracks that can be induced while tightening the screws. Additionally, graphite rods are attached to the plexiglass units as the external electrical contact points of the cell in order to transmit the applied potential to the CDI electrodes.

The CDI unit geometry is designed as vertical flow-by mode. Entrance and exit points of the feed solution in the system are located at opposite sides of the CDI unit in order to provide effective contact between the feed water and the available electrode surface, and preventing possible short-circuits in the system.

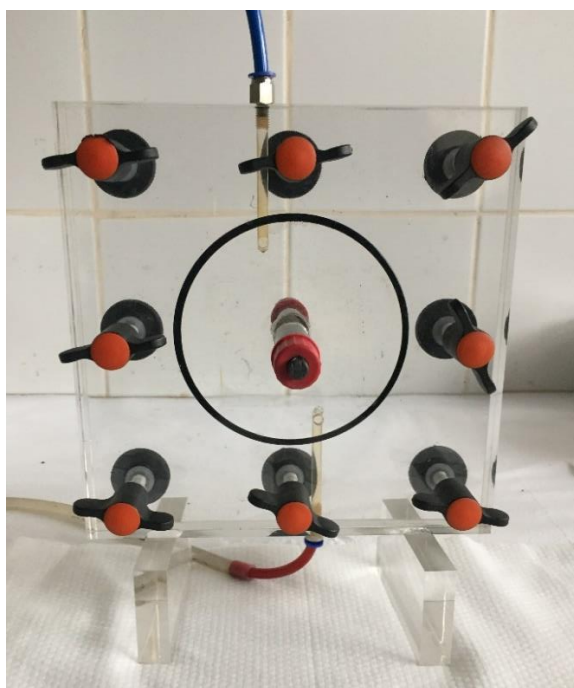


**Figure 3.1** A photograph of the lab-scale CDI unit used in the experiments.

### **3.2. Materials Used in the Experiments**

Two different carbon-based materials, namely activated carbon (AC) and graphene (GR), were used as active materials for the fabrication of electrodes during this study. They were chosen mainly because of their favorable properties, such as non-toxic nature and low cost, and easy applicability to real life applications. In addition, carbon black was used as the conductive additive, PTFE was used as the polymer binder and graphite sheets were used as the current collectors during electrode fabrication. AC was purchased from Alfa Aesar in a powder form with a particle size ranging between 425 - 850  $\mu\text{m}$ . Purchased AC was ground and sieved to obtain particles below 70  $\mu\text{m}$  prior to the fabrication of electrodes. GR was purchased from Nanografi (Turkey) in a nanoplatelet form with a purity of 99.9% with a reported flake thickness and diameter of 3 nm and 1.5  $\mu\text{m}$ , respectively (by the vendor). The conductivity of the GR is between 1,500 and 1,980 S/m. Carbon black and PTFE dispersion were obtained from Imerys and Sigma-Aldrich, respectively. All materials were used without further purification.

### 3.3. Electrode Fabrication

For the experiments, AC and GR based electrodes were used and both electrodes were fabricated using the same method. As a result of the preliminary studies, the weight ratio of active material, carbon black and PTFE in the electrodes was chosen as 80:5:15, respectively in order to provide the electrode integrity and to prevent decomposition of electrode materials into water during CDI operation. For the preparation of electrodes, first PTFE was diluted in a beaker with the addition of 10 - 15 ml ethanol as solvent. The active materials and carbon black were added to the same beaker using the aforementioned weight ratios. Prepared slurry was mixed homogeneously until it turned into a paste form and then pressed onto flexible graphite sheets (65 mm wide  $\times$  65 mm long). These graphite sheets functioned as current collectors and attachment surfaces for the prepared electrode material. Following fabrication, electrodes were dried at 80 °C for 4 h, in order to achieve complete solvent removal. A photograph of the fabricated electrode is given in Figure 3.2.

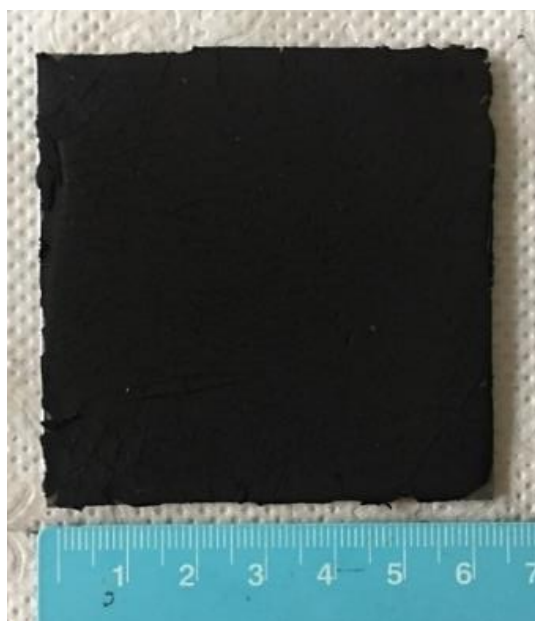


**Figure 3.2** A photograph of the fabricated electrode.

A microbalance (Sartorius Research R200D, Bradford, Germany) was used to measure the mass of fabricated electrodes. The weight of total active materials in the electrodes were measured as  $0.80 \pm 0.014$  g for each. Also, thickness of the fabricated electrodes was measured around  $350 \mu\text{m}$ , which reached to a total thickness of  $600 \mu\text{m}$  including the graphite sheet current collector. A non-electrically conductive fabric separator with a  $150 - 200 \mu\text{m}$  thickness was used in order to allow liquid to flow between the electrode couple and to prevent electrical short circuits in the system. Plexiglass plates were used to assemble the two parallel electrode sheets separated by a spacer into the CDI unit cell. Schematic configuration of the CDI unit cell is provided in Figure 3.3.

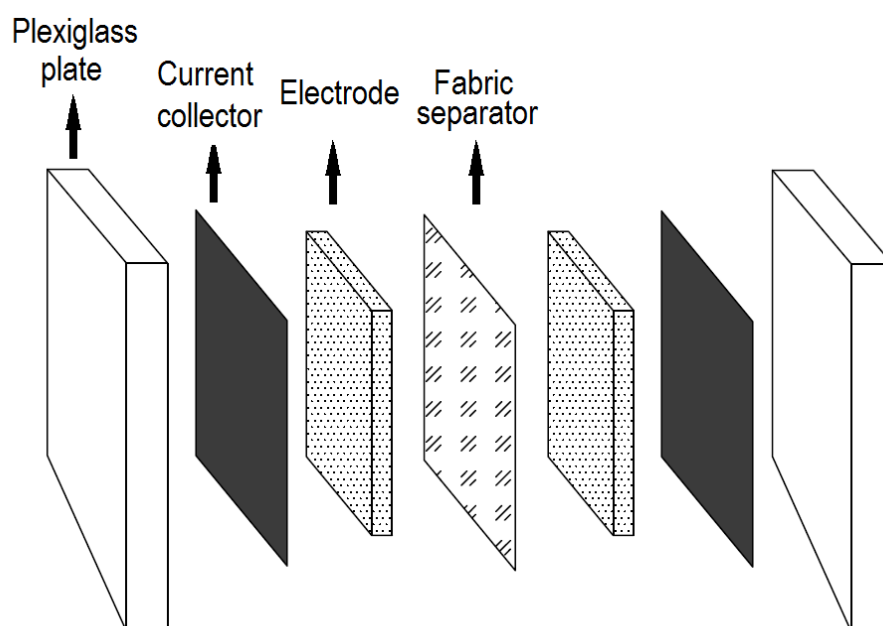


**Figure 3.3** Configuration of the CDI unit cell.

### 3.4. Material Characterizations

Electrosorptive capacities of the electrodes largely depend on characteristics of the materials used for electrode fabrication. Therefore, several characterization methods were employed on active materials used in the electrode preparation in order to understand their structural properties and chemical nature.

#### **3.4.1. Scanning Electron Microscopy (SEM)**

The structure and morphology of active carbon materials and fabricated electrodes were analysed using scanning electron microscopy (SEM, FEI Nova NanoSEM 430 microscope, operated at 10 kV). SEM samples were prepared by fixing a small amount of the material or electrode using carbon tape onto SEM specimen stubs. No additional coating was applied on the samples since they are conductive enough for the analysis.

#### **3.4.2. Transmission Electron Microscopy (TEM)**

High resolution transmission electron microscopy (HRTEM, JEOL JEM-2100F electron microscope, operated at 200 kV) was used to observe the atomic scale morphology of GR. TEM samples were prepared by suspending a small amount of GR in ethanol and drop casted onto carbon coated copper mesh grids.

#### **3.4.3. Fourier-Transform Infrared (FTIR) Spectroscopy**

In order to identify the chemical structure of GR material Fourier transform infrared spectroscopy (FTIR, Perkin Elmer 400 spectrometer, with a resolution of  $4\text{ cm}^{-1}$ ) was used. FTIR spectrum of the GR material was collected in ATR mode within a wavenumber range of  $400 - 4000\text{ cm}^{-1}$ .

#### **3.4.4. X-Ray Diffraction (XRD) Analysis**

X-Ray Diffraction (XRD, Rigaku D Max – 2000 PC diffractometer, operated at 40 kV) was used to examine the phases present and the crystal structure of the GR material. The  $2\theta$  angle varied from  $10$  to  $50^\circ$ .

#### **3.4.5. Raman Spectroscopy**

Raman spectroscopy was performed on the electrode active materials using a HORIBA Jobin Yvon iHR 550 Raman microscope with a laser wavelength of  $532\text{ nm}$ . The characteristic patterns in Raman spectrum are used to provide information about molecular vibrations, crystalline structures and orientation of the materials, and to identify substances.

### **3.4.6. Brunauer-Emmett-Teller (BET) Surface Area Analysis**

Surface characterization of the active carbon materials used in electrode fabrication was made using an Autosorp 6B system Brunauer–Emmett–Teller (BET) method was utilized to calculate the specific surface area using acquired adsorption data. In addition, pore structural properties of these materials were investigated from N<sub>2</sub> adsorption at 77 K (Quantachrome Autosorb-1, USA).

### **3.5. Electrochemical Characterizations**

In order to investigate the electrochemical behavior of the fabricated electrodes, cyclic voltammetry (CV) and galvanostatic charge discharge (GCD) analyses were performed using symmetric two electrode setup. Glass fiber was used as spacer and 1 M NaCl solution was used as electrolyte.

#### **3.5.1. Cyclic Voltammetry (CV)**

CV analysis were made in order to evaluate capacitance behavior of the fabricated electrodes, since it is an important factor for understanding the ion storage ability of a two-electrode system. Basically, CV measurement is made under a selected voltage window, where the electrode potential is scanned, and the current is recorded. It allows determination of the working voltage window of the fabricated cell and provide information about the electrochemical reaction kinetics of the electrode pairs. Electrode kinetics can be studied using different potential scan rates. Typical CV curves of a supercapacitor electrode are provided in Figure 3.4, where rectangular shape means ideal CV curve, and larger rectangle refers to a higher specific capacitance value [122].

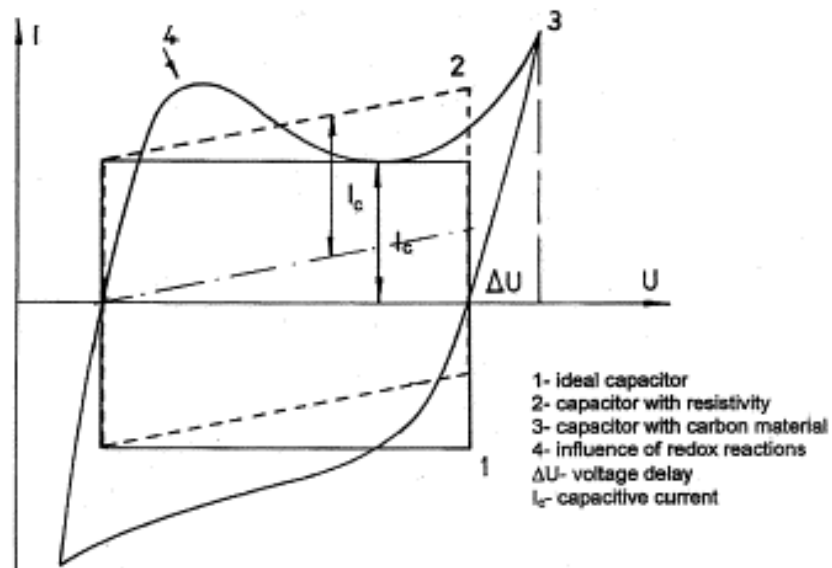


**Figure 3.4** Typical CV curve of a supercapacitor electrode [122].

### 3.5.2. Galvanostatic Charge Discharge (GCD)

GCD measurements were also made using the fabricated electrodes in order to understand their capacitance behavior and cyclic stability. In GCD analysis, constant current is applied to the cell and the obtained cell voltage is recorded with respect to time. This technique gives information about resistance, capacitance and cycle life of the fabricated electrode pairs. Typical GCD curve for a supercapacitor electrode is given in Figure 3.5, where symmetrical curve and straight lines indicate that the charging and discharging processes of the electrode materials are highly reversible. In addition, large internal resistance (IR) drop indicates high resistance in the system.

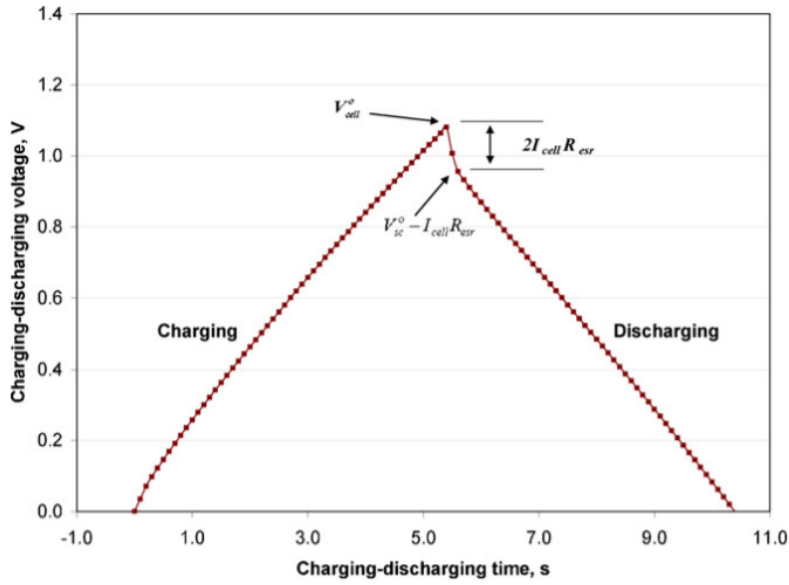


**Figure 3.5** Typical GCD curve of a supercapacitor electrode [123].

Also, specific capacitance values ( $C_{sp}$ ) of the fabricated electrodes were calculated using the obtained GCD curves and according to the formula given below [124]:

$$C_{sp} = \frac{I}{m \frac{dV}{dt}} \quad (3.1)$$

, where  $I$  is the applied discharge current (A),  $m$  is the total weight of the active material in the electrodes (g),  $V$  is the discharge voltage and  $t$  is the discharge time (s).

### 3.6. Electrosorption Experiments

Electrosorptive behavior of the fabricated electrodes was investigated in a continuously recycled batch mode system, using a CDI unit in two-electrode configuration. A peristaltic pump (Shenchen Lab2015, with flow rate capacity up to 380 ml/min) was integrated into this system to provide water flow through the CDI cell and to control the flow rate and the retention time of water in the system. In addition, a potentiostat/galvanostat system (Gamry Reference 3000) was used to apply selected voltage to the electrodes and for electrochemical measurements. A pH meter (Oakton PC2700) with a conductivity/temperature probe was used for conductivity and temperature measurements in the feed tank. The potentiostat/galvanostat and pH

meter were connected to a computer in order to control applied voltage and follow conductivity changes in the solution. Illustration of the laboratory scale CDI system is provided in Figure 3.6.

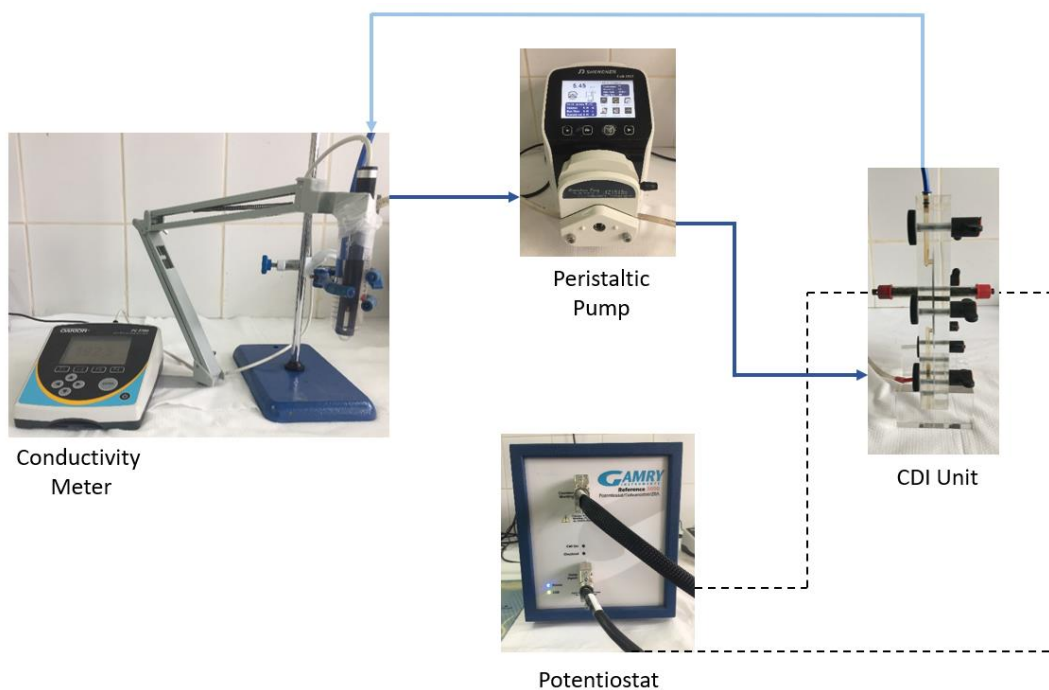


**Figure 3.6** Illustration of the laboratory scale CDI system used in the experiments.

For experiments, synthetic ionic solutions were prepared by dissolving salts with selected concentrations in deionized (DI) water. The prepared ionic solution was continuously supplied by a peristaltic pump into the CDI unit from the bottom and the effluent was collected from the top, returned to the feed tank. The feed solution was recirculated throughout the CDI unit prior to each experiment to overcome start-up effects and to achieve system stability. The volume of the feed solution was maintained as 50 ml and the temperature was kept around room temperature. After the stabilization, fabricated electrodes were charged with the selected voltage long enough to observe the electrosorption equilibrium. Lastly, for the following regeneration step, 0 V was applied to the electrodes and complete ion release was achieved. The concentration variation of the solution was continuously monitored and recorded with 30 sec time intervals using a conductivity meter. All experiments were performed in triplicate to check the reproducibility of the results.

Since the desired outcome of the desalination processes is ion removal rather than change in conductivity, calibration curves were prepared for sodium chloride (NaCl) and calcium chloride (CaCl<sub>2</sub>) salts using seven solutions with different concentrations prior to experiments in order to determine the relationship between measured conductivity and salt concentration in solutions (Figure 3.7). These were then used to calculate the concentration of ion removed from the solution by calculating the change in conductivity of the solution.

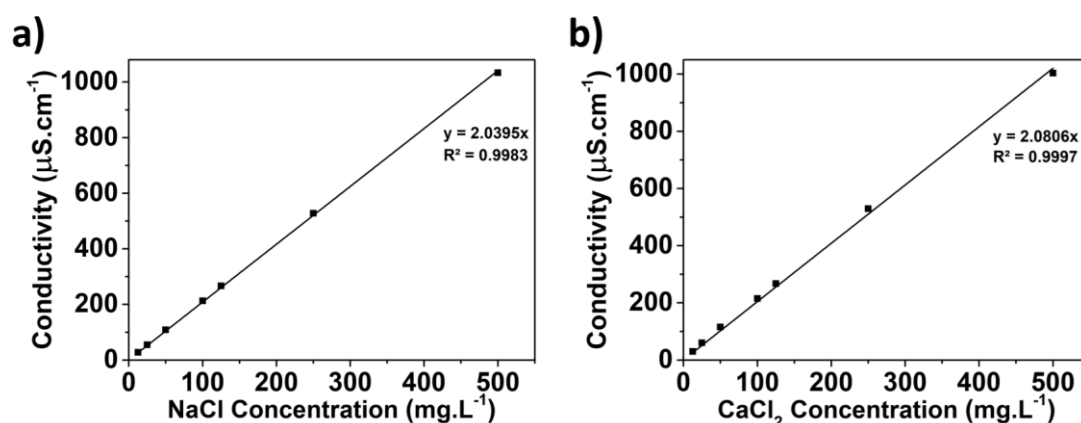


**Figure 3.7** Concentration vs conductivity calibration graphs of the (a) NaCl and (b) CaCl<sub>2</sub> salts used in the CDI experiments.

At the end of the experiments, electrosorptive capacity (EC) of the fabricated electrodes was calculated using the equation [125]:

$$\text{Electrosorptive Capacity} \left[ \frac{\mu\text{mol}}{\text{g}} \right] = d \times \left[ \frac{(C_0 - C) \times V_{\text{sol}}}{(M \times MW)} \right] \quad (3.2)$$

, where  $C$  and  $C_0$  represent the final and initial salt concentrations in the water (mg/l), respectively,  $V$  is the volume of the feed solution (ml),  $M$  is the mass of active material in the fabricated electrodes (g),  $d$  is the valence electron number of the salt ion in the feed solution and  $MW$  is the molecular weight of the salt (g/mol) used in the experiments.

### **3.6.1. Effect of System Operation Parameters on Electrosorptive Capacity**

The effect of flow rate and working voltage on electrosorptive capacity of the fabricated AC and GR based electrodes were investigated in order to determine the optimum operation parameters for both electrodes in the prepared CDI system. For the experiments, three different flow rates (5, 10, 20 ml/min) and three different voltages (1.6, 1.8, 2.0 V) were chosen as the testing parameters based on the literature. Experiments were performed using a synthetic NaCl solution with an initial concentration of 100 ppm, which has a conductivity around 215  $\mu\text{S}/\text{cm}$ ; and charge time of the electrodes were chosen as 4 hr. At the end of the experiments, optimum operation parameters were obtained based on the highest electrosorptive capacity achieved. Following experiments were conducted using these optimum flow rate and applied voltage parameters.

### **3.6.2. Effect of Ion Type and Concentration on Electrosorptive Capacity**

Electrosorptive capacities of the fabricated AC and GR based electrodes were also investigated using different ionic solutions with different concentrations in order to determine their selective ion removal mechanism. For the experiments, monovalent NaCl and divalent  $\text{CaCl}_2$  salts were used to prepare solutions at concentrations of 50, 100 and 200 ppm, which had conductivities around 108, 215 and 425  $\mu\text{S}/\text{cm}$ , respectively. In addition, control experiments were conducted using only DI water as feed water to the CDI unit. System operation parameters were chosen according to the previous experiment and the charge time of the electrodes were chosen as 4 hrs.

### **3.6.3. Regeneration of the Fabricated Electrodes**

Cyclic generation and regeneration of the fabricated AC and GR based electrodes were performed in order to investigate their long term use and reversibility. The experiments were performed using 100 ppm NaCl solution as the feed water, and the water flow rate and applied voltage were chosen according to optimization experiment

results. The generation time of the electrodes were chosen as 120 min in each cycle of the experiments in order to decrease the process time and total of 20 cycles were collected sequentially for each electrode.

## CHAPTER 4

### RESULTS AND DISCUSSIONS

#### 4.1. Characterization of the Materials Used in CDI Electrodes

Morphology of the AC powder and GR used in the experiments as active materials for the fabrication of electrodes was investigated using SEM analysis. SEM images of the AC powder and GR are provided in Figure 4.1 (a) and (b), respectively. From the SEM images, it was observed that the particle size below 70  $\mu\text{m}$  was achieved for AC as a result of the previous grinding process. In fact, the sample mostly consisted of particulates in the size range of 20 – 50  $\mu\text{m}$ . In addition, it is shown that GR has homogeneous, 3D structure mostly in nanoscale, and it consists of stacked platelet forms. Therefore, the GR will be referred to as graphene-like material (GLM) throughout the thesis.

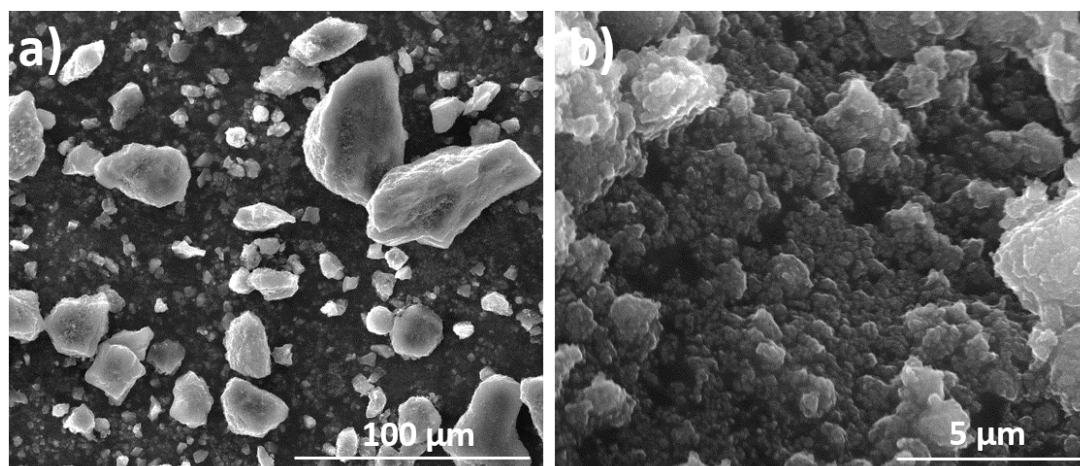


**Figure 4.1** SEM images of (a) AC powder and (b) GLM used in the CDI electrodes.

Detailed morphological characterization of the commercially available GLM was done using TEM, FTIR and XRD analyses. Graphitic fringes can be seen from TEM images (Figure 4.2 (a) and (b)) and it was observed that GLM consists of small and

defective multi-layers. The FTIR spectrum of GLM is provided in Figure 4.2 (c), data between wavenumbers of 1800 – 2300  $\text{cm}^{-1}$  were omitted from the graph since they showed peaks related to ATR crystal used during analysis. GLM showed two peaks at wavenumbers of 1517  $\text{cm}^{-1}$  and 1675  $\text{cm}^{-1}$ , which represent the existence of graphitic domains and aromatic C=C bonds in the material. Peaks at 2845  $\text{cm}^{-1}$ , 2913  $\text{cm}^{-1}$  and 2957  $\text{cm}^{-1}$  represent the C-H stretch vibrations of methylene group in the material [126]. GLM also had an O-H stretching vibration band at 3565  $\text{cm}^{-1}$  and 3614  $\text{cm}^{-1}$ , and C-O stretching vibration at 1089  $\text{cm}^{-1}$ . XRD pattern of GLM showed two peaks at  $2\theta$  values of 26.40° and 43.60° as shown in Figure 4.2 (d). These peaks correspond to (002) and (100) diffraction planes of graphitic origin of the GLM. The considerable broadening in the diffraction peaks can be attributed to the defective nature of the non-uniformly distributed multilayers [127].

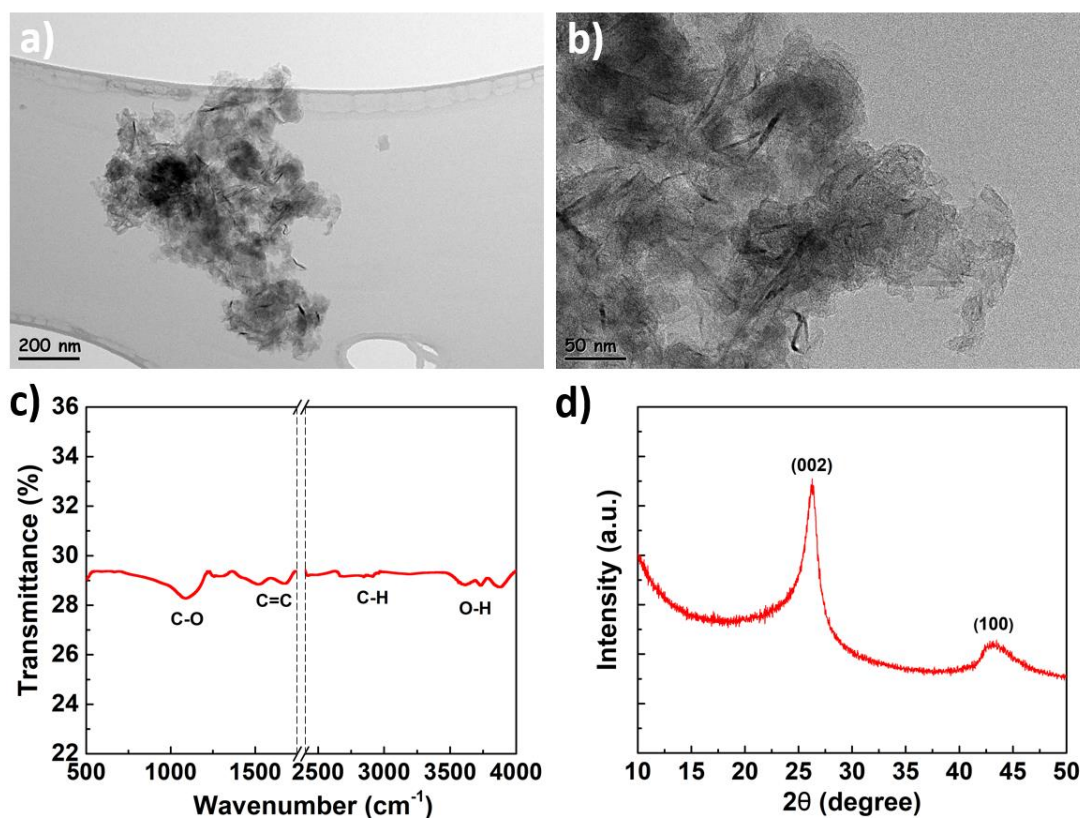


**Figure 4.2** (a) Low magnification and (b) high magnification TEM images and (c) FTIR spectrum and (d) XRD pattern of the GLM used in the CDI electrodes.

Chemical nature of the carbon based electrode active materials was investigated using Raman spectroscopy. Obtained Raman spectrums of AC and GLM in a wavenumber range from 1000 to 3000  $\text{cm}^{-1}$  are provided in Figure 4.3. These results show that both materials show two peaks at around 1350  $\text{cm}^{-1}$  (D band, the defects and disordered band) and 1600  $\text{cm}^{-1}$  (G band, the ordered graphitic band). The intensity ratio of D and G bands ( $I_D/I_G$ ) represents the magnitude of defects in the material. Smaller  $I_D/I_G$  ratio is an indicative of a high graphitization degree.  $I_D/I_G$  value was calculated as 1.58 and 1.26 for the AC and GLM materials, respectively. These results indicated that GLM had slightly more ordered graphite crystallites compared to AC. Generally, improved graphitization degree of carbon materials leads to higher electrical conductivity which would be helpful for improving the desalination performance of the CDI process [128]. On the other hand, higher  $I_D/I_G$  value of the AC demonstrates that it has more defects and functional groups, which is believed to be beneficial to the charge transfer in electrosorption process [31]. In addition, GLM shows a third peak at around 2710  $\text{cm}^{-1}$  (2D band), which is related to the number of layers in material. 2D peak represents the graphene-like nature of the material rather than graphite, which shows a 2D peak with two components at around 2750  $\text{cm}^{-1}$  [129]. Also, the lower intensity of 2D band compared to other peaks can be attributed to the presence of multilayers in GLM, which could offer higher adsorption capacity [130].

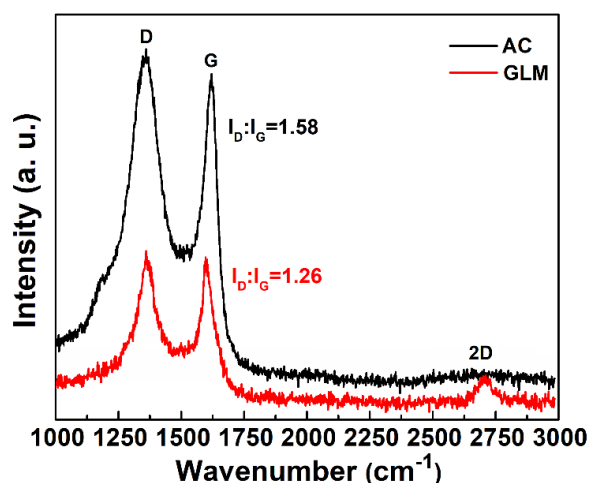


**Figure 4.3** Raman spectra of AC powder and GLM used in the fabrication of CDI electrodes.

The nitrogen (N<sub>2</sub>) adsorption–desorption isotherms and the pore size distributions of AC and GLM were analyzed and the obtained results are presented in Figure 4.4. From the Figure 4.4 (a), it is observed that both carbon materials show a typical type-IV isotherm with a hysteresis loop between the adsorption and desorption steps at a relative pressure of  $P/P_0 > 0.5$ , which is consistent with mesoporous structure of the material and indicates the existence of some mesopores. Also, the maximum N<sub>2</sub> adsorption quantity of GLM is approaching to 900 cm<sup>3</sup>/g and considerably higher than that of AC, which is around 500 cm<sup>3</sup>/g, implying that the specific adsorption area of GLM is much higher than that of AC. In addition, the pore size distribution analysis of the carbon materials (Figure 4.4 (b)) revealed that AC mostly consisted of micropores and GLM is mainly in mesoporous range (2 – 50 nm). The measured pore size of GLM is mainly attributed to the interlayer gaps between the GLM, which is different from AC. Parameters such as surface area and pore volume of the materials are provided in the table inserted in Figure 4.4 (b). The surface area and the volume of micropores associated with GLM are smaller than mesopores, which is vice versa for AC. Considering these results together with the pore size distributions (shown in Figure 4.4 (b)), it can be stated that GLM comprises of a larger fraction of mesopores when compared to AC, which would ensure presence of reasonable space for ion adsorption during CDI process.

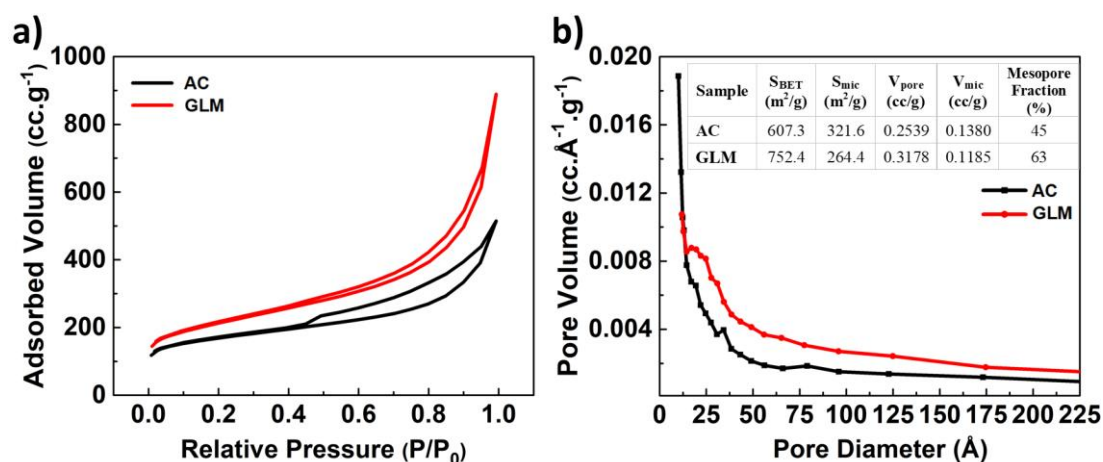


**Figure 4.4** (a) Nitrogen adsorption-desorption isotherms and (b) pore size distributions of the AC powder and GLM used for the CDI electrodes.

## 4.2. Characterization of the Fabricated CDI Electrodes

Surface and cross section morphologies of the fabricated AC and GLM based electrodes were investigated using SEM analysis. The SEM images of the as-prepared (non-used) electrodes including their cross-sectional views are provided in Figure 4.5. From the images, it was observed that both of the fabricated electrodes are homogeneous and show a porous structure, which allows the easy accessibility of the feed solution into inner pores of the electrodes. In addition, the density of GLM electrode seems quite high, which may limit rapid ion removal. It is also possible to see especially from the cross-sectional images shown in the inset of Figure 4.5 (a) and (b) that the AC electrodes mainly consist of irregular porous structure, while the GLM electrodes show multilayered structure. Furthermore, it is possible to observe that no excessive amount of binders exists on surface of the fabricated electrodes, and the binder act as a web-like structure between the electrode materials, holding them together and is essential to form the electrode integrity. However, pore blocking/filling effect of polymeric binders could also decrease the advantages of carbon materials, reducing ion adsorption capacity.

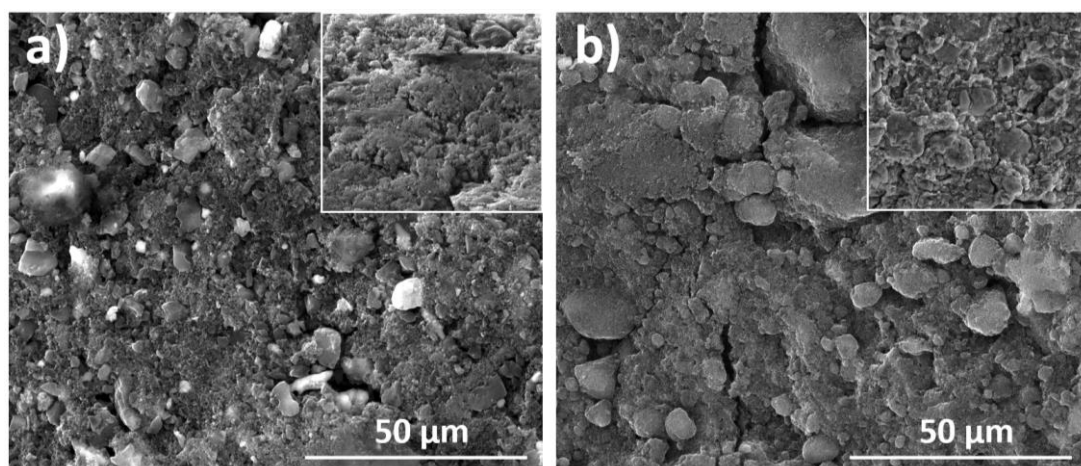


**Figure 4.5** SEM images of the (a) AC and (b) GLM based freshly prepared (non-used) electrodes. Insets show the cross-sectional images of the electrodes.

CV measurements were conducted to evaluate the electrochemical performance of the fabricated AC and GLM based electrodes using a two-electrode cell at room temperature, using a 1 M NaCl solution as the electrolyte. For the experiments voltage windows of 0 - 1.6 V, 0 - 1.8 V and 0 - 2.0 V, and scan rates of 50, 100 and 200 mV were tested. CV results for AC and GLM based electrodes are provided in Figure 4.6.

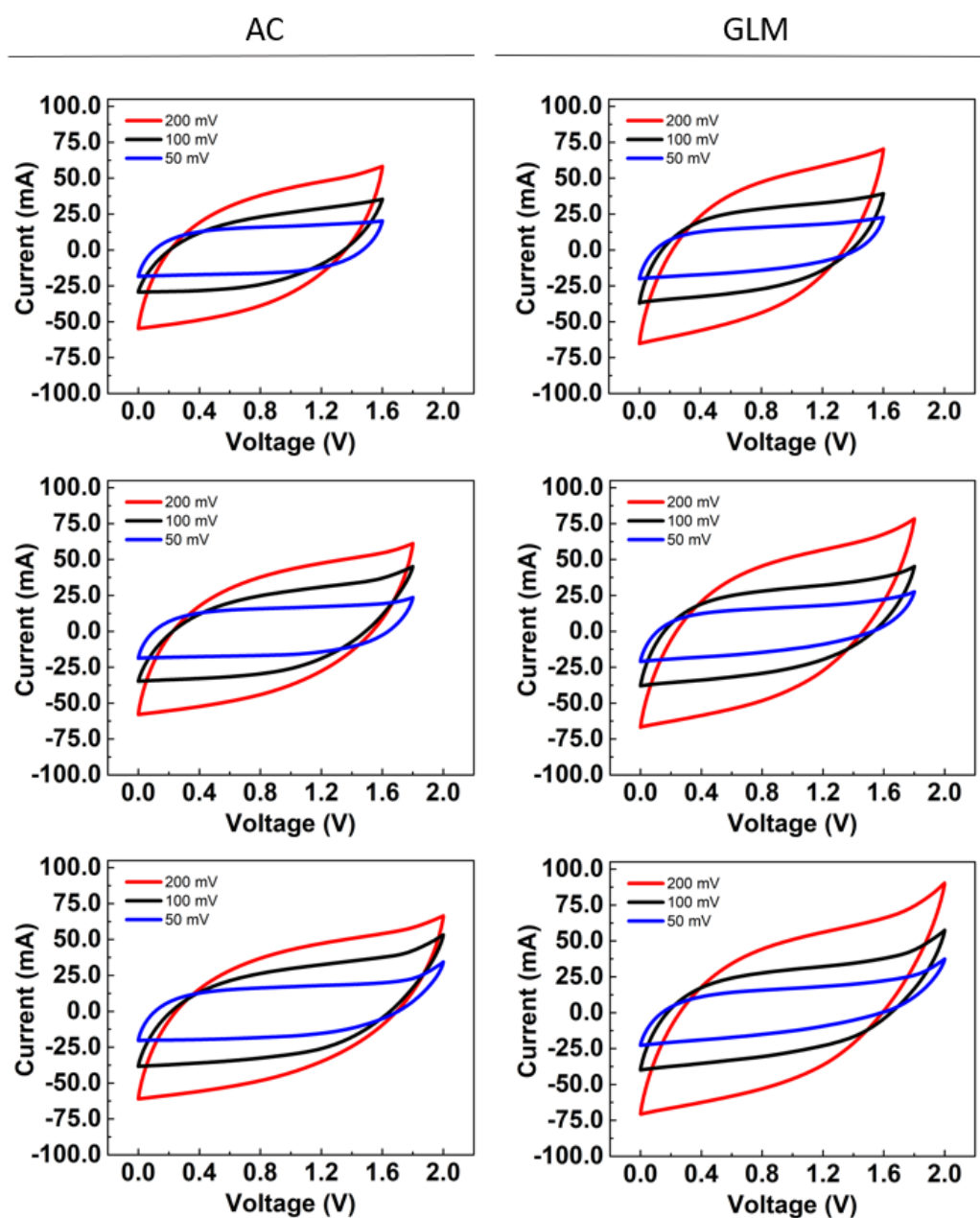


**Figure 4.6** CV analysis results for AC and GLM based electrodes using voltage windows of (a,b) 1.6 V, (c,d) 1.8 V and (e,f) 2.0 V, respectively.

As a result of the CV analyses, both electrodes show a symmetrical rectangular-like shape and there are no redox peaks observed in any of the curves, indicating that the results derive from EDL capacitance rather than Faradaic capacitance. Also, it was observed that both electrodes have a better CV (rectangle) shape at the scan rate of 50 mV. The CV results at 50 mV scan rate with varying voltage windows are given in Figure 4.7; comparative results for AC and GLM based electrodes at 50 mV scan rate and 0 - 2.0 V voltage window are provided in Figure 4.8.

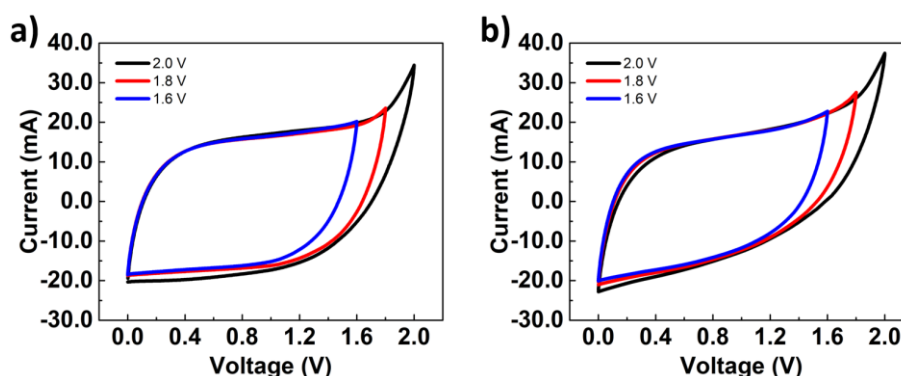


**Figure 4.7** CV analysis results for (a) AC and (b) GLM based electrodes using a scan rate of 50 mV and varying voltage windows.

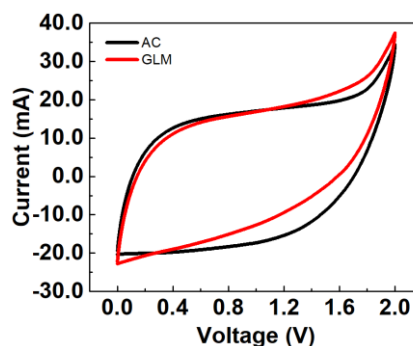


**Figure 4.8** Comparative CV analysis results for AC and GLM based electrodes using 50 mV scan rate and 0 - 2.0 V voltage window.

As shown in Figure 4.7 (a) and (b), the rectangular shape of AC is better than that of GLM for all voltage windows indicating that fabricated AC electrodes were highly ideal as supercapacitor electrodes. Also, it was observed that GLM electrodes show slight resistance probably because of their dense morphology. In addition, Figure 4.8 shows that the CV curve area of the fabricated electrodes are similar to each other; hence, close specific capacitance values was expected for the both electrodes.

GCD analyses were also conducted for better understanding of electrochemical behavior of the fabricated AC and GLM based electrodes in two-electrode system configuration at room temperature, where a 1 M NaCl solution was served as the electrolyte. For the experiments three applied currents of 50, 75 and 100 mA and voltage windows of 0 - 1.6 V, 0 - 1.8 V and 0 - 2.0 V were used. GCD results for AC and GLM based electrodes are given in Figure 4.9.

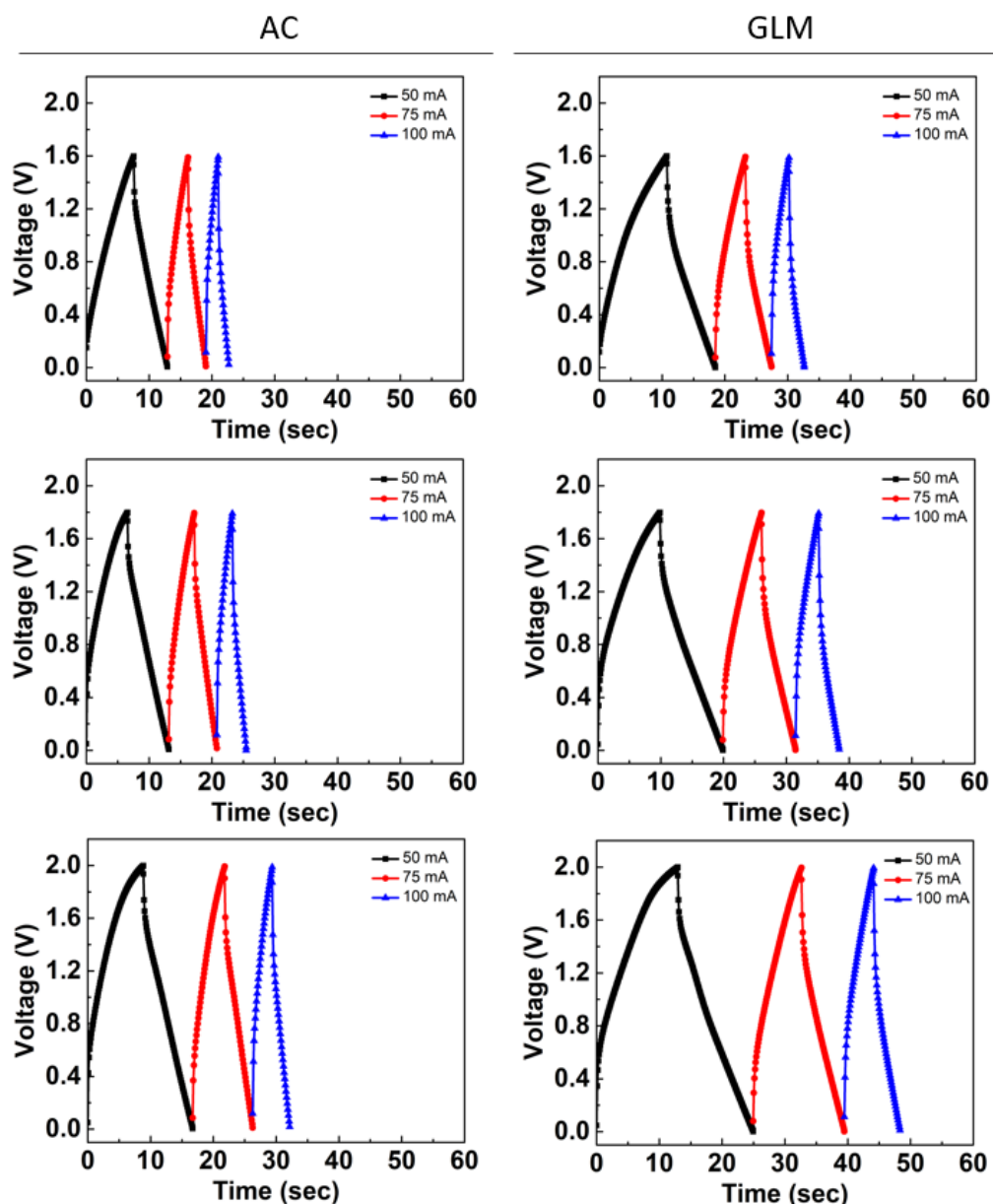


**Figure 4.9** GCD analysis results for AC and GLM based electrodes at different voltages of (a,b) 1.6 V, (c,d) 1.8 V and (e,f) 2.0 V, respectively.

As a result of the GCD analyses, both electrodes show a typical triangular shape, indicating favorable charge/discharge properties and a good EDL capacitance. Also, IR drop was observed for both electrodes at all experiments, which indicates the internal resistance of fabricated electrodes. This is probably because of the use of polymeric binder and low quantity of carbon black in the fabrication of electrodes. In addition, it was observed that both electrodes have better curves at specific current of 50 mA. Specific capacitance values of the fabricated electrodes were calculated with respect to applied currents of 50, 75 and 100 mA at 0 - 2.0 V voltage window, and obtained results are provided in Figure 4.10.

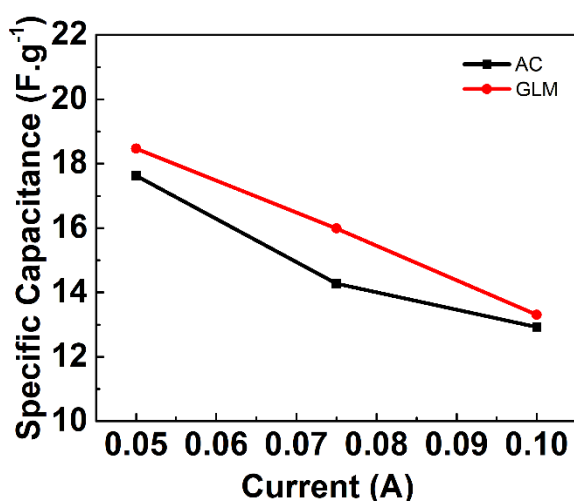


**Figure 4.10** Calculated specific capacitance values of the fabricated electrodes with respect to applied currents of 50, 75 and 100 mA and at 0 - 2.0 V voltage window.

From Figure 4.10, it was observed that the specific capacitance of GLM based electrodes is higher than AC based electrodes at all scan rates, probably due to the mesoporous structure of GLM, which provides more proper adsorption sites for ions, and because of the hydrophobicity of AC resulted by its microporous structure, which results the volume of pores could not be utilized completely. In addition, specific capacitance values decreased with increasing scan rates for both electrodes. The specific capacitance values decreased from 17.6 F/g to 12.9 F/g for AC based electrodes and from 18.5 F/g to 13.3 F/g for GLM based electrodes.

### 4.3. Electrosorption Experiments

#### 4.3.1. Effect of Water Flow Rate and Applied Voltage

Effect of flow rate and applied voltage on the ion removal efficiency of the fabricated AC and GLM electrodes were investigated in the CDI unit. Changes of solution ion concentration with respect to time for flow rates of 5, 10 and 20 ml/min are provided in Figure 4.11. Error bars represent reproducibility of triplicate experiments.

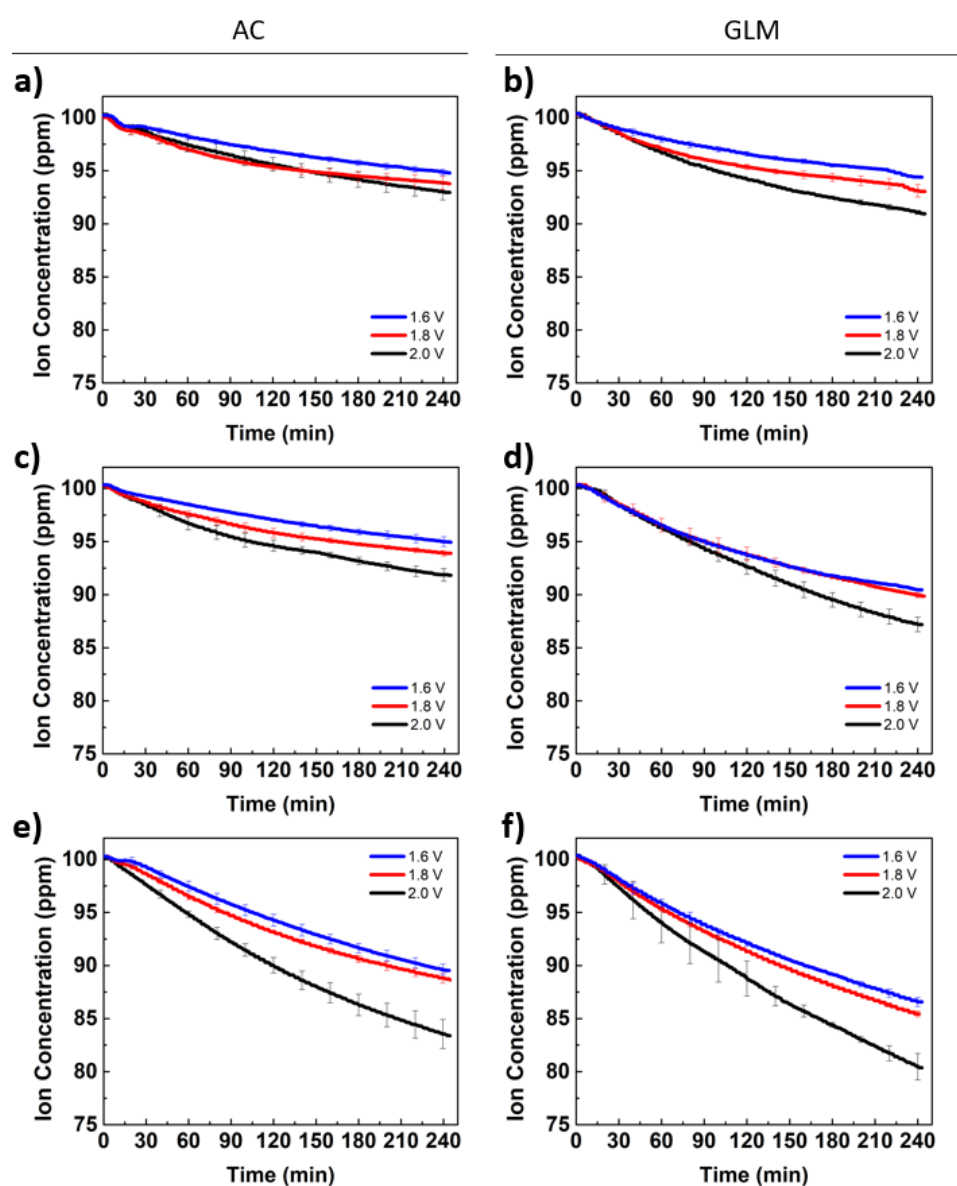


**Figure 4.11** Results of electrosorption experiments for AC and GLM based electrodes at a flow rate of (a,b) 5 ml/min, (c,d) 10 ml/min and (e,f) 20 ml/min.

During all experiments, upon the application of the selected voltage at time=0, conductivity of the ionic solutions started to decrease immediately for both electrodes and under all operating conditions. The conductivity decrease continued throughout the operation time, which implied that both electrodes can operate under these operational conditions without perceptible deterioration. Water electrolysis (bubble formation) was not observed during the experiments under the selected operational parameters. Average electrosorptive capacities (EC) of the electrodes were calculated for all experiments and the results are provided in Figure 4.12 (a) and (b) for AC and GLM based electrodes, respectively.

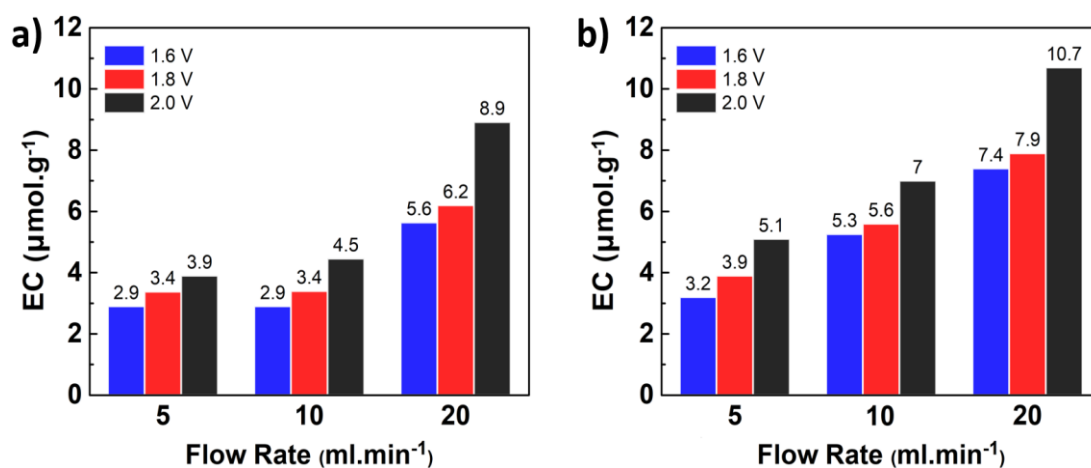


**Figure 4.12** Average electrosorptive capacities of (a) AC and (b) GLM based electrodes based on different flow rates and applied voltages.

According to Figure 4.12, increasing flow rates resulted in a higher degree of ion removal for both AC and GLM based electrodes. This can be attributed to the force created by the turbulent flow at high flow rates, which may facilitate the electrosorption of ions in the porous structure of the CDI electrodes [131]. In addition, at high flow rates, mixing of the solution was improved and the CDI system was loaded with a stadier concentration gradient, which might have caused higher ion transfer onto the electrodes [131]. As seen from Figure 4.12 (a), ion adsorption capacities of AC based electrodes were nearly the same at low flow rates of 5 and 10  $\text{ml/min}$ , and at 20  $\text{ml/min}$  flow rate the capacities got almost doubled for all applied

voltages. This is probably because of the microporous structure of the AC, which made it difficult for the feed solution to reach deeper layers and prevented complete wetting of the AC electrodes at low flow rates [132], causing prevention of the use of surface in micropores for ion adsorption. For flow rates of 5 and 10 ml/min, the flow rate was not effective enough to increase the ion adsorption capacity of the AC based electrodes. Besides, at higher flow rates (i.e. 20 ml/min) with increasing turbulent flow effect in the system, it became possible to reach more available pores, and thus ion adsorption capacity of the AC based electrodes increased significantly.

As seen from Figure 4.12 (b), ion adsorption capacities of the GLM electrodes increased at a steady pace with increasing water flow rate and related turbulent flow in the system. This was probably because mesoporous structure of GLM allowed feed solution to reach the available pores of the fabricated electrodes relatively more easily and electrode wetting was achieved even at lower flow rates. Therefore, ion adsorption capacity of the GLM based electrodes was not significantly limited by the water flow rate. Also, increasing water flow rate in the system enhanced the use of available multilayers of GLM for ion adsorption and thus, the highest amount of ion adsorption was observed at the highest flow rate of 20 ml/min.

Furthermore, the difference between 5, 10 and 20 ml/min flow rates was more explicit at higher potentials. The ion adsorption capacities of both AC and GLM based electrodes were enhanced as applied voltage increased and reached its maximum value of 8.9  $\mu\text{mol/g}$  and 10.7  $\mu\text{mol/g}$  at 2.0 V, respectively. This indicated that the increasing applied voltage enhanced the electrostatic forces on surface of the electrodes, leading to the formation of a thicker EDL [112], and thus more ions were adsorbed on the electrode. Experiments were not continued using higher applied potentials, since water hydrolysis was observed at an applied voltage of 2.1 V during preliminary experiments. Considering the results of this experiment, following experiments were conducted using fixed operational parameters of flow rate and applied voltage as 20 ml/min and 2.0 V, respectively, which were the operational parameters resulted in the highest ion adsorption capacities.

### 4.3.2. Effect of Ion Type and Concentration in the Feed Water

Effects of the salt concentration and valence number of the ions in the feed solution on ion adsorption performance of the fabricated AC and GLM electrodes were also investigated in the CDI unit. Changes of solution ion concentration with respect to time for initial salt concentrations of 50, 100 and 200 ppm are provided in Figure 4.13. Error bars represent reproducibility of triplicate experiments.

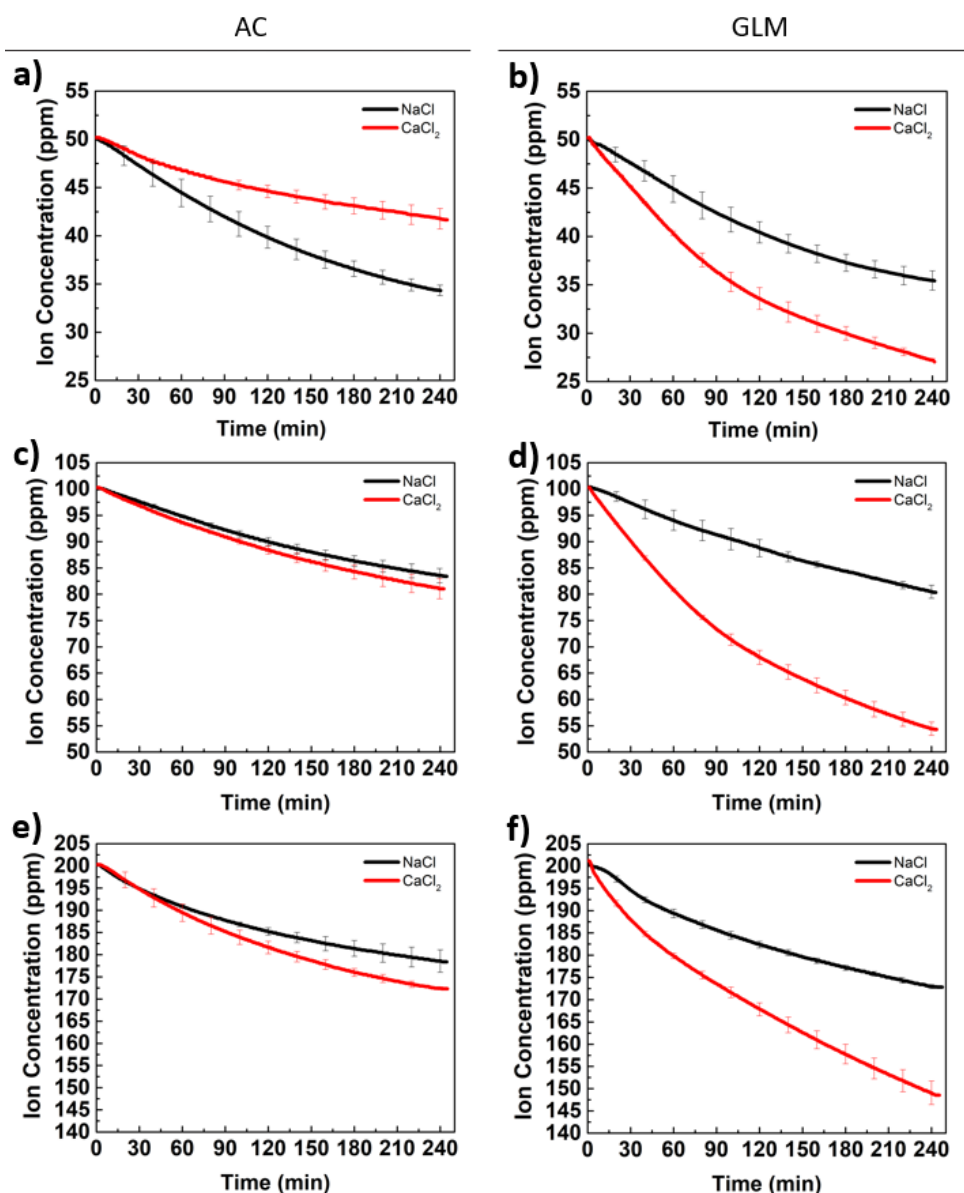


**Figure 4.13** Results of electrosorption experiments for AC and GLM based electrodes using a feed solution salt concentration of (a,b) 50 ppm, (c,d) 100 ppm and (e,f) 200 ppm.

According to the obtained results shown in Figure 4.13, following the application of 2.0 V (at time=0), conductivity of the ionic solutions started to continuously decrease and this decrease continued throughout the experiments for the both electrodes similar to the previous results. This indicated that the use of both salts with all selected initial salt concentrations have no limiting effect on the ion adsorption of the system. In addition, control experiments where only DI water was used as a feed water to the CDI unit (Figure 4.14) showed no significant change in ion concentration (ion removal or ion release from the electrode materials) for both electrodes.

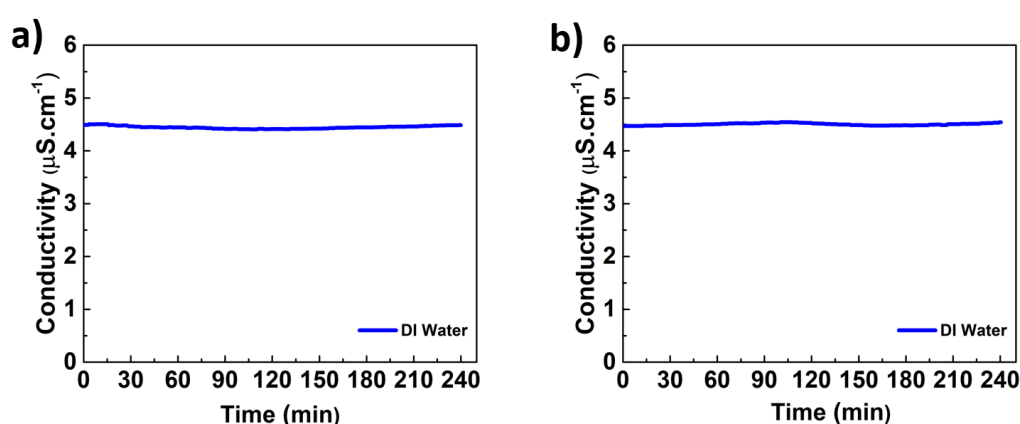


**Figure 4.14** Results of control experiments for (a) AC and (b) GLM based electrodes using DI water as a feed solution.

At the end of the all experiments average electrosorptive capacities of the electrodes were calculated, and the results are provided in Figure 4.15 (a) and (b) for AC and GLM based electrodes, respectively. As a result of these experiments, it was observed that the electrosorptive capacities of AC and GLM based electrodes for both salts increased with the initial salt concentration of the feed solutions. One of the possible reasons for that was the increase in conductivity in the highly concentrated solutions, which enhanced electrostatic forces between the electrodes and electrochemical properties of the system as well as the ion removal efficiencies. In addition, because of the greater concentration gradient in highly concentrated solutions, ions can easily transport through the pores and got adsorbed by the electrodes [125]. The salt concentration of the feed solution also significantly affected the diffuse double-layer

capacity of the fabricated electrodes, which was an important factor for enhancing the electrosorptive capacity. The capacity of diffuse double-layer increased with the salt concentration in electrolyte solution [116]. Hence, the electrosorptive capacity of the both fabricated electrodes were found to increase at higher salt concentrations.

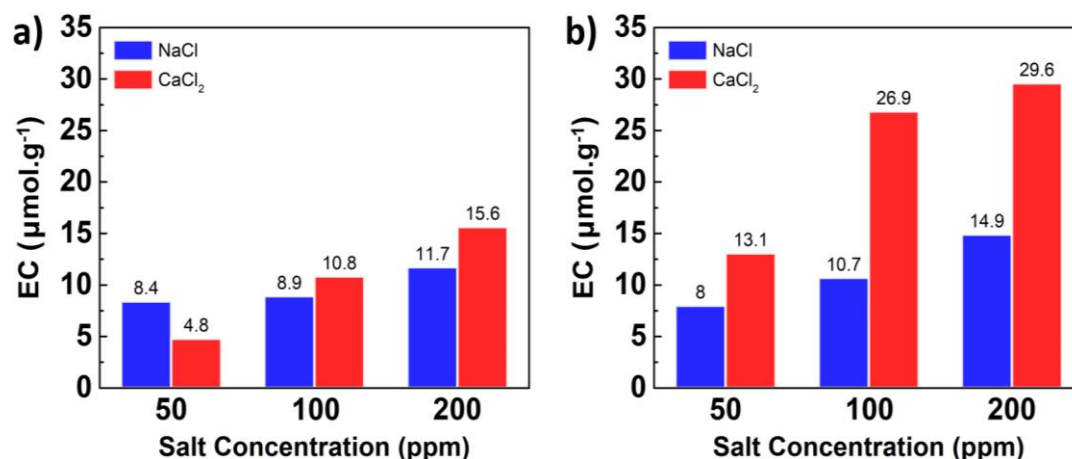


**Figure 4.15** Average electrosorptive capacities of (a) AC and (b) GLM based electrodes based on different flow rates and applied voltages.

In addition, at lower salt concentrations (50 ppm), higher electrosorptive capacities were observed for monovalent ions ( $\text{Na}^+$ ) compared to divalent ions ( $\text{Ca}^{2+}$ ) for the AC electrodes, which indicated higher removal efficiency. This is probably because of the fact that ions with a lower charge can be adsorbed/transported in the micropores of the AC electrodes much easier due to their small hydrated radius [24]. This seemed to be in effect at lower salt concentrations, where the electrostatic forces were not that dominant as compared to physical adsorption. Although ions with higher valence had more restrictions to penetrate into the pores of the electrodes, it is well known that they have stronger Coulombic interactions with the charged electrode surface [125]. Therefore, at higher salt concentrations (100 and 200 ppm) with enhanced electrostatic force, divalent ions were more effectively removed from the solution compared to the monovalent ions; and electrosorptive capacity of  $\text{Na}^+$  and  $\text{Ca}^{2+}$  ions reached 11.7 and 15.6  $\mu\text{mol/g}$ , respectively at concentration of 200 ppm. The obtained results demonstrate that for AC electrode with microporous structure the hydrated radius of

ion has a stronger effect on ion adsorption than the ionic charge at lower salt concentrations where the electrostatic forces are weak. However, at higher salt concentrations multivalent  $\text{Ca}^{2+}$  had a considerably higher capacity compared to monovalent  $\text{Na}^+$  with a strong dependence on ionic charge.

On the other hand, for the GLM based electrodes with mesoporous structure, ion removal capacities for  $\text{Ca}^{2+}$  ions were found higher than that for  $\text{Na}^+$  ions for all experiments. This difference doubled at higher salt concentrations with enhancing electrostatic forces and reached 14.9 and 29.6  $\mu\text{mol/g}$ , respectively at concentration of 200 ppm. These results showed that electrosorption capacity of the ions is highly dependent on the initial concentration and valence number of the ions rather than the hydrated radius. This is a limiting factor for the AC based electrodes with microporous structure to achieve higher  $\text{Ca}^{2+}$  removal, especially at lower salt concentrations.

According to the results of similar studies in the literature, achieved electrosorptive capacities of pure carbon based CDI electrodes for NaCl removal were found as 5.73  $\mu\text{mol/g}$  [133], 7.7  $\mu\text{mol/g}$  [31], 16.9  $\mu\text{mol/g}$ , 18.8  $\mu\text{mol/g}$  [90], 25.8  $\mu\text{mol/g}$ , 30.8  $\mu\text{mol/g}$  [9] and 31.6  $\mu\text{mol/g}$  [56]. The highest capacity observed in this study for NaCl removal was 11.7  $\mu\text{mol/g}$  for AC electrodes and 14.9  $\mu\text{mol/g}$  for GLM electrodes. In addition, to our knowledge there is one similar study investigated  $\text{CaCl}_2$  removal in literature [31], and as a result of this study electrosorptive capacity of 9.91  $\mu\text{mol/g}$  was achieved. The highest capacity observed in this study for  $\text{CaCl}_2$  removal was 15.6  $\mu\text{mol/g}$  for AC electrodes and 29.6  $\mu\text{mol/g}$  for GLM electrodes. The results of this study are comparable with the similar studies. Table 4.1 is prepared to compare obtained results in this work with those in literature concerning carbon based CDI electrodes with reported ECs. It is clear that the obtained results in this work are highly promising.

**Table 4.1** A comparison of CDI results of this study and similar studies with carbon based electrodes from literature.

Electrode Material	Salt Type	EC ( $\mu\text{mol/g}$ )	Reference
AC	NaCl	11.7	This study
GLM	NaCl	14.9	
AC	NaCl	5.73	[133]
GR	NaCl	7.7	[31]
AC	NaCl	16.9	[90]
GR	NaCl	18.8	
AC	NaCl	25.8	[9]
GR	NaCl	30.8	
GR	NaCl	31.6	[56]
AC	CaCl <sub>2</sub>	15.6	This study
GLM	CaCl <sub>2</sub>	29.6	
GR	CaCl <sub>2</sub>	9.91	[31]

In addition, various results were obtained regarding different electrode materials used in CDI applications (Table 2.1). Most of these CDI studies conducted with materials synthesized specifically for the use in the CDI process using pure, laboratory grade materials. These fabrication methods can be very time consuming and expensive. This study on the other hand achieved comparable results to some of these results using commercially available, environmentally friendly and cost-efficient carbon materials, which can be operated at wide applied potential ranges and show promising ion removal performance. These properties should also be taking into consideration for possible real life and long term CDI applications of these materials.

#### 4.3.3. Regeneration of the Fabricated CDI Electrodes

Regeneration experiments were made with the fabricated AC and GLM electrodes in order to understand their stability during the CDI operation. The experiments were performed using a water flow rate and applied voltage of 20 ml/min and 2.0 V, respectively. Conductivity of the feed solution was measured and recorded with respect to time throughout the experiments. Regeneration test results of the AC and

GLM electrodes are provided in Figure 4.16. The first three cycles of the experiments were considered to allow the fabricated electrodes to stabilize and get completely wet, thus they were omitted from the graph for better understanding of the long term behavior of AC and GLM based electrodes.

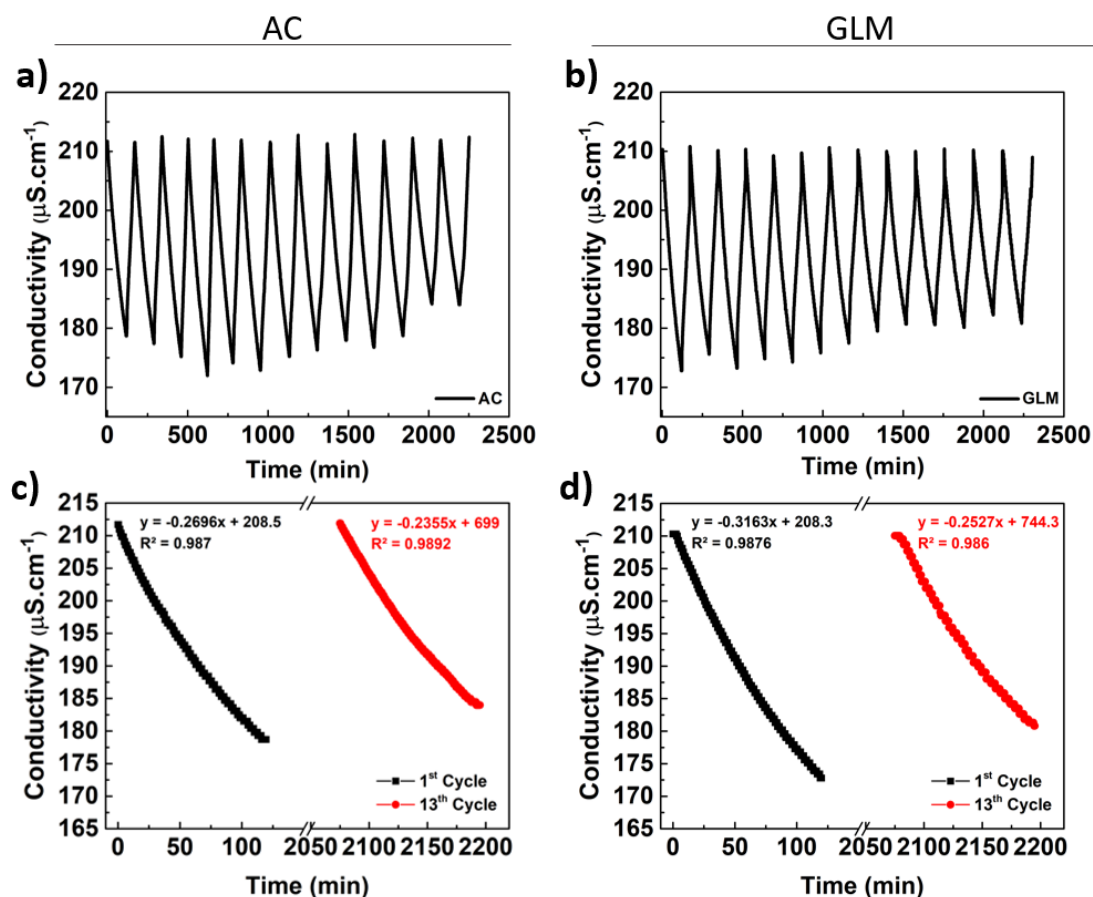


**Figure 4.16** Regeneration test results of the AC and GLM based electrodes, showing: (a, b) all cycles and (c,d) comparison of first and last cycles.

It is evident from the Figure 4.16 (a) and (b) that following the stabilization of the system, conductivity of the solution decreased during the charge step and then can reach back to the initial value at the discharge step for all cycles. In order to better depict change in electrosorptive performance of the system, the first and last cycles are re-plotted for better visibility (Figure 4.16 (c) and (d)). It was observed that electrosorption curves show slight change in slope. This may indicate high and

reversible capacity retention of the fabricated CDI electrodes. For AC electrodes, slope of the charge steps changed between -0.2235 and -0.3212 with a median value of -0.2895, and for GLM electrodes, slope of the charge steps changed between -0.2227 and -0.3163 with a median value of -0.2715. However, after several cycles the ion removal capacity of the fabricated electrodes started to decrease slowly. This might be due to either a decrease in the ion adsorption capacity of the fabricated electrodes or increase in the process time to reach the equilibrium. Nevertheless, the fabricated AC and GLM electrodes show good potential to be used many times in the CDI process.

In addition, SEM images of the fabricated AC and GLM based electrodes after regeneration were obtained in order to investigate the changes in electrode morphology following CDI application. The SEM images of the regenerated (used) electrodes are provided in Figure 4.17. It was observed from the SEM images that after long term use and complete wetting of the fabricated electrodes in a continuously fed CDI system, their porous structure became more visible. This explains the steadier electrosorptive capacities reached following stabilization of the electrodes. In addition, dense morphology of non-used GLM electrodes was not observed from used electrodes, which is a probable result of the expansion of multilayer structure of GLM with the effect of continuous water flow in the system. Although there are some slight changes on the morphological properties of the electrodes, there was no significant pore blockage, corrosion or fouling on the surface of the used electrodes that might negatively affect the CDI process efficiency.

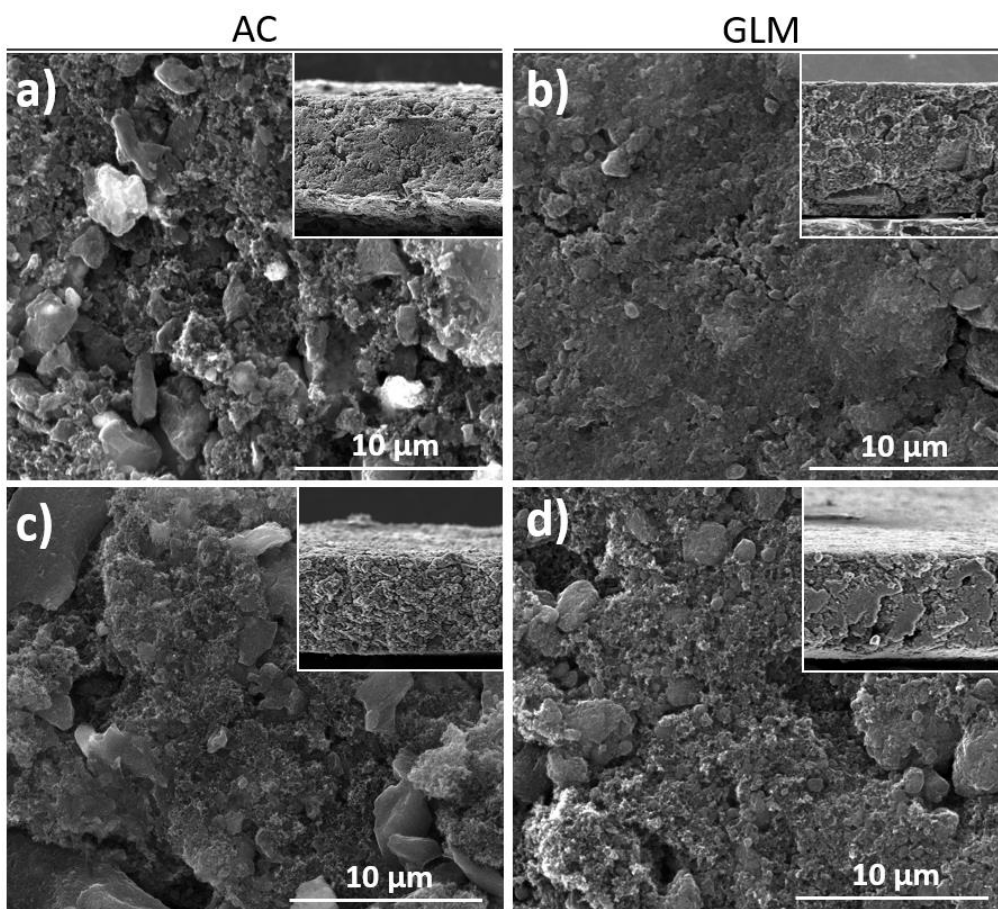


**Figure 4.17** SEM images of the AC and GLM based electrodes (a,b) before and (c,d) following CDI process. Insets show the cross-sectional images of the electrodes.

## CHAPTER 5

### CONCLUSIONS

In this study, ion removal performance of the CDI process was investigated under various operating conditions. For this purpose, AC and GLM based electrodes were fabricated using commercially available materials and their characterizations were made. Deionization performance of the fabricated AC and GLM electrodes was investigated using a laboratory scale CDI unit. Ion adsorption behavior of the fabricated electrodes with different structural properties was analyzed at different electrical potentials and water flow rates, and using feed solutions with different initial salt concentration and ionic species. Main conclusions obtained from this study are listed below.

- Pore size of AC is mainly in microporous range while GLM mostly consisted of mesopores.
- The fabricated AC and GLM electrodes were homogeneous and show a porous structure. Also, some pore blocking/filling effect of polymeric binder (PTFE) was observed.
- The ion adsorption capacities of both AC and GLM based electrodes were enhanced with the water flow rate. Highest ion removal rate was obtained at the highest flow rate of 20 ml/min. At low flow rates, microporous structure of AC made it difficult for the feed solution to reach deeper layers and caused prevention of the use of whole electrode surface for ion adsorption. On the other hand, ion adsorption capacity of the GLM based electrodes was not significantly limited by the water flow rate.

- The ion adsorption capacities of both AC and GLM based electrodes were enhanced with the applied voltage and reached their maximum value of 8.9  $\mu\text{mol/g}$  and 10.7  $\mu\text{mol/g}$ , respectively, at a flow rate of 20 ml/min and an applied potential of 2.0 V.
- For AC based electrode with microporous structure the hydrated radius of ion had a stronger effect on the ion adsorption compared to the ionic charge at lower concentrations and higher electro sorptive capacities were observed for monovalent ( $\text{Na}^+$ ) ions than divalent ( $\text{Ca}^{2+}$ ) ions. However, at higher salt concentrations divalent ions had a considerably higher capacity than that of monovalent ions, showing strong dependence on ionic charge. On the other hand, for the GLM based electrodes with mesoporous structure, electro sorption capacity of the ions was highly dependent on the valence of the ions rather than the hydrated radius. Ion removal capacities for divalent ions were higher than that for monovalent ions at all concentrations.
- The electro sorptive capacities of AC and GLM based electrodes were found to increase with initial salt concentration of the feed solution and reached their maximum value of 11.7 and 14.9  $\mu\text{mol/g}$  for  $\text{Na}^+$  ions, and 15.6 and 29.6  $\mu\text{mol/g}$  for  $\text{Ca}^{2+}$  ions, respectively at the highest tested salt concentration of 200 ppm.
- The fabricated AC and GLM based electrodes exhibited advantageous reversibility, and there was no significant pore blockage, corrosion or fouling on the surface of the used electrodes which would otherwise negatively affect the CDI process efficiency with repetitive use.

## CHAPTER 6

### RECOMMENDATIONS FOR FUTURE STUDIES

CDI technology is a promising alternative for deionization/desalination applications, especially considering the process cost and energy efficiency and environmental concerns. Thus, extending the knowledge in this area and improvement of the literature is important. The results of this study contribute to the base knowledge in the literature about comparative CDI process performance of carbon electrodes with different structural properties depending on various operational parameters. Considering the conclusions of this study, following points can be taken into consideration for future studies.

- Electrode fabrication methods can be improved without the need for materials that may adversely affect the ion removal capacity of CDI electrodes, such as polymeric binders.
- Deionization performance of the CDI process using more complex solutions with competing ions and different anions including different pollutants like heavy metals can be investigated for fully understanding of the behavior of CDI electrodes and extending the process applicability.
- Materials with different morphology may show different ion removal efficiencies for specific pollutants depending on water quality. Considering decreasing salt concentration of water with time while in CDI system, combining different electrodes that show different ion removal behavior in a CDI stack unit can be investigated in order to decrease material the cost and increase efficiency of the CDI unit.

- In real world applications, CDI systems must be able to operate for as long as possible. Thus, a systematic study on the long term performance of the CDI process should be conducted for practical applications.
- Detailed cost analysis of the CDI process should be done using real life case studies in order to better compare the CDI technology with conventional desalination technologies.

## REFERENCES

- [1] A. S. Yasin, H. O. Mohamed, I. M. Mohamed, H. M. Mousa and N. A. Barakat, "Enhanced desalination performance of capacitive deionization using zirconium oxide nanoparticles-doped graphene oxide as a novel and effective electrode," *Separation and Purification Technology*, vol. 171, p. 34–43, 2016.
- [2] G. Rasines, P. Lavela, P. Macias, M. C. Zafra, J. L. Tirado and C. O. Ania, "On the use of carbon black loaded nitrogen-doped carbon aerogel for the electrosorption of sodium chloride from saline water," *Electrochimica Acta*, vol. 170, p. 154–163, 2015.
- [3] H. Li, L. Zou, L. Pan and Z. Sun, "Novel Graphene-Like Electrodes for Capacitive Deionization," *Environmental Science & Technology*, vol. 44, p. 8692–8697, 2010.
- [4] "The United Nations World Water Development Report," UNESCO, France, 2018.
- [5] V. G. Gude, "Desalination and Sustainability – An Appraisal and Current Perspective," *Water Research*, vol. 89, pp. 87-106, 2016.
- [6] N. Hassan, "Ground Water Depletion Due To Water Mining – A Threat," *Journal of Environmental Science, Computer Science and Engineering & Technology*, vol. 5, pp. 129 - 136, 2016.
- [7] S. Porada, R. Zhao, A. van der Wal, V. Presser and P. M. Biesheuvel, "Review on the science and technology of water desalination by capacitive deionization," *Progress in Materials Science*, vol. 58, p. 1388–1442, 2013.

- [8] F. A. AlMarzooqi, A. A. Al Ghaferi, I. Saadat and N. Hilal, "Application of Capacitive Deionisation in water desalination: A review," *Desalination*, vol. 342, pp. 3 - 15, 2014.
- [9] Z. Wang, B. Dou, L. Zheng, G. Zhang, Z. Liu and Z. Hao, "Effective desalination by capacitive deionization with functional graphene nanocomposite as novel electrode material," *Desalination*, vol. 299, p. 96–102, 2012.
- [10] United Nations, "Clean Water and Sanitation: Why It Matters," 2016.
- [11] T. Humplik, J. Lee, S. C. O'Hern, B. A. Fellman, M. A. Baig, S. F. Hassan, M. A. Atieh, F. Rahman, T. Laoui, R. Karnik and E. N. Wang, "Nanostructured materials for water desalination," *Nanotechnology*, vol. 22, pp. 1-19, 2011.
- [12] R. Danoun, "Desalination Plants: Potential impacts of brine discharge on marine life," The University of Sydney, Australia, 2007.
- [13] A. Subramani and J. G. Jacangelo, "Emerging desalination technologies for water treatment: A critical review," *Water Research*, vol. 75, pp. 164-187, 2015.
- [14] P. Reig, A. Maddocks and F. Gassert, "World's 36 Most Water-Stressed Countries," 12 12 2013. [Online]. Available: <https://www.wri.org/blog/2013/12/world-s-36-most-water-stressed-countries>. [Accessed 05 10 2018].
- [15] A. Maddocks, R. S. Young and P. Reig, "Ranking the World's Most Water-Stressed Countries in 2040," 26 08 2015. [Online]. Available: <https://www.wri.org/blog/2015/08/ranking-world-s-most-water-stressed-countries-2040>. [Accessed 05 10 2018].

- [16] S. Manju and N. Sagar, "Renewable energy integrated desalination: A sustainable solution to overcome future fresh-water scarcity in India," *Renewable and Sustainable Energy Reviews*, vol. 73, pp. 594-609, 2017.
- [17] L. Wang, Y. Zhou, J. Wang and N. Hu, "Approaching Capacitive Deionization (CDI) on Desalination of Water and Wastewater -New Progress and Its Potential," *Advanced Materials Research*, vol. 1088, pp. 557-561, 2015.
- [18] "Glossary of Salt Water," Water Quality Association, 2008.
- [19] J. Liu, S. Wang, J. Yang, J. Lao, M. Lu, H. Pan and L. An, "ZnCl<sub>2</sub> activated electrospun carbon nanofiber for capacitive desalination," *Desalination*, vol. 344, p. 446–453, 2014.
- [20] A. Uyduranoğlu Öktem and A. Aksoy, "Türkiye'nin Su Riskleri Raporu," World Wildlife Fund - Turkey, İstanbul, 2014.
- [21] O. Lefebvre and R. Moletta, "Treatment of organic pollution in industrial saline wastewater: A literature review," *Water Research*, vol. 40, pp. 3671 - 3682, 2006.
- [22] L. Zou, G. Morris and D. Qi, "Using activated carbon electrode in electrosorptive deionisation of brackish water," *Desalination*, vol. 225, p. 329–340, 2008.
- [23] P. Liang, L. Yuan, X. Yang, S. Zhou and X. Huang, "Coupling ion-exchangers with inexpensive activated carbon fiber electrodes to enhance the performance of capacitive deionization cells for domestic wastewater desalination," *Water Research*, vol. 47, pp. 2523-2530, 2013.
- [24] S.-J. Seo, H. Jeon, J. K. Lee, G.-Y. Kim, D. Park, H. Nojima, J. Lee and S.-H. Moon, "Investigation on removal of hardness ions by capacitive

- deionization (CDI) for water softening applications," *Water Research*, vol. 44, p. 2267–2275, 2010.
- [25] A. G. El-Deen, N. A. Barakat and H. Y. Kim, "Graphene wrapped MnO<sub>2</sub>-nanostructures as effective and stable electrode materials for capacitive deionization desalination technology," *Desalination*, vol. 344, pp. 289-298, 2014.
- [26] "Guidelines for Water Reuse," U.S. Environmental Protection Agency, 2012.
- [27] World Health Organization (WHO), "Guidelines for Drinking-water Quality," 2011. [Online]. Available: [http://apps.who.int/iris/bitstream/handle/10665/44584/9789241548151\\_eng.pdf;jsessionid=3F6632AAFFC6D18D2CAA40F72B5F201A?sequence=1](http://apps.who.int/iris/bitstream/handle/10665/44584/9789241548151_eng.pdf;jsessionid=3F6632AAFFC6D18D2CAA40F72B5F201A?sequence=1). [Accessed 06 10 2018].
- [28] A. Bennett, "50th anniversary: Desalination: 50 years of progress," *Filtration + Separation*, vol. 50, pp. 32-39, 2013.
- [29] "Desalination by the Numbers," International Desalination Association, [Online]. Available: <http://idadesal.org/desalination-101/desalination-by-the-numbers/>. [Accessed 05 10 2018].
- [30] T. J. Welgemoed and C. F. Schutte, "Capacitive Deionization Technology™: An alternative desalination solution," *Desalination*, vol. 183, pp. 327 - 340, 2005.
- [31] H. Li, L. Zou, L. Pan and Z. Sun, "Using graphene nano-flakes as electrodes to remove ferric ions by capacitive deionization," *Separation and Purification Technology*, vol. 75, p. 8–14, 2010.

- [32] T. N. Tuan, S. Chung, J. K. Lee and J. Lee, "Improvement of water softening efficiency in capacitive deionization by ultra purification process of reduced graphene oxide," *Current Applied Physics*, vol. 15, pp. 1397-1401, 2015.
- [33] M. T. Z. Myint, S. H. Al-Harhi and J. Dutta, "Brackish water desalination by capacitive deionization using zinc oxide micro/nanostructures grafted on activated carbon cloth electrodes," *Desalination*, vol. 344, p. 236–242, 2014.
- [34] E. García-Quismondo, C. Santos, J. Lado, J. Palma and M. A. Anderson, "Optimizing the Energy Efficiency of Capacitive Deionization Reactors Working under Real-World Conditions," *Environmental Science and Technology*, vol. 47, pp. 11866 - 11872, 2013.
- [35] M. A. Anderson, A. L. Cudero and J. Palma, "Capacitive deionization as an electrochemical means of saving energy and delivering clean water. Comparison to present desalination practices: Will it compete?," *Electrochimica Acta*, vol. 55, p. 3845–3856, 2010.
- [36] D. Dursun, S. Ozkul, R. Yuksel and H. E. Unalan, "Enhancing capacitive deionization technology as an effective method for water treatment using commercially available graphene," *Water Science and Technology*, vol. 75, pp. 643 - 649, 2017.
- [37] M. A. Ahmed and S. Tewari, "Capacitive deionization: Processes, materials and state of the technology," *Journal of Electroanalytical Chemistry*, vol. 813, p. 178 – 192, 2018.
- [38] L. L. Zhang and X. S. Zhao, "Carbon-based materials as supercapacitor electrodes," *Chemical Society Reviews*, vol. 38, pp. 2520 - 2531, 2009.
- [39] B. Jia and W. Zhang, "Preparation and Application of Electrodes in Capacitive Deionization (CDI): a State-of-Art Review," *Nanoscale Research Letters*, 2016.

- [40] Y. Oren, "Capacitive deionization (CDI) for desalination and water treatment - past, present and future (a review)," *Desalination*, vol. 228, pp. 10 - 29, 2008.
- [41] T. Brousse, D. Belanger and J. W. Long, "To Be or Not To Be Pseudocapacitive?," *Journal of The Electrochemical Society*, vol. 162, pp. 5158-5189, 2015.
- [42] C. Zhang, D. He, J. Ma, W. Tang and T. D. Waite, "Faradaic reactions in capacitive deionization (CDI) - problems and possibilities: A review," *Water Research*, no. 128, pp. 314 - 330, 2018.
- [43] "Web of Science Database Report," Clarivate Analysis, [Online]. Available: <https://www.webofknowledge.com>. [Accessed 16 01 2019].
- [44] M. Mossad, W. Zhang and L. Zou, "Using capacitive deionisation for inland brackish groundwater desalination in a remote location," *Desalination*, no. 308, pp. 154 - 160, 2013.
- [45] W. Zhang, M. Mossad and L. Zou, "A study of the long-term operation of capacitive deionisation in inland brackish water desalination," *Desalination*, vol. 320, pp. 80-85, 2013.
- [46] T.-H. Yu, H.-Y. Shiu, M. Lee, P.-T. Chiueh and C.-H. Hou, "Life cycle assessment of environmental impacts and energy demand for capacitive deionization technology," *Desalination*, vol. 399, pp. 53-60, 2016.
- [47] L. Weinstein and R. Dash, "Capacitive Deionization: Challenges and Opportunities," *Desalination & Water Reuse*, pp. 34 - 37, 2013.
- [48] A. Altaee and N. Hilal, "High Recovery Rate NF-FO-RO Hybrid System for Inland Brackish Water Treatment," *Desalination*, vol. 363, pp. 19-25, 2015.

- [49] L. Y. Lee, H. Y. Ng, S. L. Ong, G. Tao, K. Kekre, B. Viswanath, W. Lay and H. Seah, "Integrated pretreatment with capacitive deionization for reverse osmosis reject recovery from water reclamation plant," *Water Research*, no. 43, pp. 4769 - 4777, 2009.
- [50] C. Santos, J. J. Lado, E. García-Quismondo, I. V. Rodriguez, D. Hospital-Benito, J. Palma, M. A. Anderson and J. J. Vilatela, "Interconnected metal oxide CNT fibre hybrid networks for current collector-free asymmetric capacitive deionization," *Journal of Materials Chemistry A*, vol. 6, 2018.
- [51] Y. Bai, Z.-H. Huang, X.-L. Yu and F. Kang, "Graphene oxide-embedded porous carbon nanofiber webs by electrospinning for capacitive deionization," *Colloids and Surfaces A: Physicochemical and Engineering Aspects*, vol. 444, p. 153–158, 2014.
- [52] M. S. Gaikwad and C. Balomajumder, "Capacitive Deionization for Desalination Using Nanostructured Electrodes," *Analytical Letters*, vol. 49, no. 11, p. 1641–1655, 2016.
- [53] J. Oladunni, J. H. Zain, A. Hai, F. Banat, G. Bharath and E. Alhseinat, "A comprehensive review on recently developed carbon based nanocomposites for capacitive deionization: From theory to practice," *Separation and Purification Technology*, vol. 207, p. 291 – 320, 2018.
- [54] J.-H. Choi, "Fabrication of a carbon electrode using activated carbon powder and application to the capacitive deionization process," *Separation and Purification Technology*, vol. 70, pp. 362-366, 2010.
- [55] S.-W. Bian, Y.-P. Zhao and C.-Y. Xian, "Porous MnO<sub>2</sub> hollow spheres constructed by nanosheets and their application in electrochemical capacitors," *Materials Letters*, vol. 111, pp. 75-77, 2013.

- [56] H. Li, T. Lu, L. Pan, Y. Zhang and Z. Sun, "Electrosorption behavior of graphene in NaCl solutions," *Journal of Materials Chemistry*, vol. 19, p. 6773–6779, 2009.
- [57] E. Avraham, B. Yaniv, A. Soffer and D. Aurbach, "Developing Ion Electroadsorption Stereoselectivity, by Pore Size Adjustment with Chemical Vapor Deposition onto Active Carbon Fiber Electrodes. Case of Ca<sup>2+</sup>/Na<sup>+</sup> Separation in Water Capacitive Desalination," *The Journal of Physical Chemistry*, vol. 112, no. 19, pp. 7385-7389, 2008.
- [58] H.-J. Oh, J.-H. Lee, H.-J. Ahn, Y. Jeong, J.-H. Kim and C.-H. Chi, "Nanoporous activated carbon cloth for capacitive deionization of aqueous solution.," *Thin Solid Films*, vol. 515, pp. 220-225, 2006.
- [59] I. Cohen, E. Avraham, M. Noked, A. Soffer and D. Aurbach, "Enhanced charge efficiency in capacitive deionization achieved by surface-treated electrodes and by means of a third electrode.," *The Journal of Physical Chemistry C*, vol. 115, pp. 19856-19863, 2011.
- [60] A. Aghigh, V. Alizadeh, H. Y. Wong, M. S. Islam, N. Amin and M. Zaman, "Recent advances in utilization of graphene for filtration and desalination of water: A review," *Desalination*, vol. 365, pp. 389-397, 2015.
- [61] L. L. Song, Z. Aruna, J. S. Guo and B. Z. Jang, "Nano-scaled graphene plate nanocomposites for supercapacitor electrodes". US Patent 11/499,861, 2006.
- [62] H. Wang, D. Zhang, T. Yan, X. Wen, J. Zhang, L. Shi and Q. Zhong, "Three-dimensional macroporous graphene architectures as high performance electrodes for capacitive deionization," *Journal of Materials Chemistry A*, vol. 1, p. 11778 – 11789, 2013.
- [63] H. Duan, T. Yan, Z. An, J. Zhang, L. Shi and D. Zhang, "Rapid construction of 3D foam-like carbon nanoarchitectures via a simple photochemical

- strategy for capacitive deionization," *RSC Advances*, vol. 7, p. 39372–39382, 2017.
- [64] P. Liu, H. Wang, T. Yan, J. Zhang, L. Shi and D. Zhang, "Grafting sulfonic and amine functional groups on 3D graphene for improved capacitive deionization," *Journal of Materials Chemistry A*, vol. 14, pp. 5303 - 5313, 2016.
- [65] J. Biener, M. Stadermann, M. Suss, M. A. Worsley, M. M. Biener, K. A. Rose and T. F. Baumann, "Advanced carbon aerogels for energy applications," *Energy and Environmental Science*, vol. 4, p. 656 – 667, 2011.
- [66] H. Li, L. Pan, T. Lu, Y. Zhan, C. Nie and Z. Sun, "A comparative study on electrosorptive behavior of carbon nanotubes and graphene for capacitive deionization," *Journal of Electroanalytical Chemistry*, vol. 653, p. 40–44, 2011.
- [67] H. Li, Y. Ma and R. Niu, "Improved capacitive deionization performance by coupling TiO<sub>2</sub> nanoparticles with carbon nanotubes," *Separation and Purification Technology*, vol. 171, pp. 93-100, 2016.
- [68] A. G. El-Deen, J.-H. Choi, C. S. Kim, K. A. Khalil, A. A. Almajid and N. A. Barakat, "TiO<sub>2</sub> nanorod-intercalated reduced graphene oxide as high performance electrode material for membrane capacitive deionization," *Desalination*, vol. 361, pp. 53-64, 2015.
- [69] J. Yang, L. Zou, H. Song and Z. Hao, "Development of novel MnO<sub>2</sub>/nanoporous carbon composite electrodes in capacitive deionization technology," *Desalination*, vol. 276, p. 199–206, 2011.
- [70] E. Raymundo-Pinero, V. Khomenko, E. Frackowiak and F. Beguin, "Performance of Manganese Oxide/CNTs Composites as Electrode Materials

- for Electrochemical Capacitors," *Journal of the Electrochemical Society*, vol. 152, pp. 229-235, 2005.
- [71] V. Augustyn, P. Simon and B. Dunn, "Pseudocapacitive oxide materials for high-rate electrochemical energy storage," *Energy & Environmental Science*, vol. 7, p. 1597–1614, 2014.
- [72] J. Liu, M. Lu, J. Yang, J. Cheng and W. Cai, "Capacitive desalination of ZnO/activated carbon asymmetric capacitor and mechanism analysis," *Electrochimica Acta*, vol. 151, p. 312–318, 2015.
- [73] A. G. El-Deen, N. A. Barakat, K. A. Khalil, M. Motlak and H. Y. Kim, "Graphene/SnO<sub>2</sub> nanocomposite as an effective electrode material for saline water desalination using capacitive deionization," *Ceramics International*, vol. 40, p. 14627–14634, 2014.
- [74] C. Kim, J. Lee, S. Kim and J. Yoon, "TiO<sub>2</sub> sol–gel spray method for carbon electrode fabrication to enhance desalination efficiency of capacitive deionization," *Desalination*, vol. 342, p. 70–74, 2014.
- [75] L. M. Chang, X. Y. Duan and W. Liu, "Preparation and electrosorption desalination performance of activated carbon electrode with titania," *Desalination*, vol. 270, pp. 285 - 290, 2011.
- [76] A. Thamilselvan, A. S. Nesaraj and M. Noel, "Review on carbon-based electrode materials for application in capacitive," *International Journal of Environmental Science and Technology*, vol. 13, pp. 2961 - 2976, 2016.
- [77] C. Yan, L. Zou and R. Short, "Polyaniline-modified activated carbon electrodes for capacitive deionisation," *Desalination*, vol. 333, p. 101–106, 2014.

- [78] Y. Wang, L. Zhang, Y. Wu, S. Xu and J. Wang, "Polypyrrole/carbon nanotube composites as cathode material for performance enhancing of capacitive deionization technology," *Desalination*, vol. 354, pp. 62 - 67, 2014.
- [79] X. Gu, Y. Yang, Y. Hu, M. Hu, J. Huang and C. Wang, "Facile fabrication of graphene–polypyrrole–Mn composites as high-performance electrodes for capacitive deionization," *Journal of Materials Chemistry A*, vol. 3, p. 5866 – 5874, 2015.
- [80] L. Zou, L. Li, H. Song and G. Morris, "Using mesoporous carbon electrodes for brackish water desalination," *Water Research*, vol. 42, pp. 2340-2348, 2008.
- [81] C.-H. Hou, J.-F. Huang, H.-R. Lin and B.-Y. Wang, "Preparation of activated carbon sheet electrode assisted electrosorption process," *Journal of the Taiwan Institute of Chemical Engineers*, vol. 43, pp. 473 - 479, 2012.
- [82] Z. Chen, C. Song, X. Sun, H. Guo and G. Zhu, "Kinetic and isotherm studies on the electrosorption of NaCl from aqueous solutions by activated carbon electrodes," *Desalination*, vol. 267, pp. 239 - 243, 2011.
- [83] Y.-J. Kim and J.-H. Choi, "Enhanced desalination efficiency in capacitive deionization with an ion-selective membrane," *Separation and Purification Technology*, vol. 71, pp. 70-75, 2010.
- [84] H. H. Jung, S. W. Hwang, S. H. Hyun, K. H. Lee and G. T. Kim, "Capacitive deionization characteristics of nanostructured carbon aerogel electrodes synthesized via ambient drying," *Desalination*, vol. 216, p. 377–385, 2007.
- [85] J. C. Farmer, D. V. Fix, G. V. Mack, R. W. Pekala and J. F. Poco, "Capacitive Deionization of NaCl and NaNO<sub>3</sub> Solutions with Carbon Aerogel Electrodes," *Journal of Electrochemical Society*, vol. 143, pp. 159-169, 1996.

- [86] L. Wang, M. Wang, Z.-H. Huang, T. Cui, X. Gui, F. Kang, K. Wang and D. Wu, "Capacitive deionization of NaCl solutions using carbon nanotube sponge electrodes," *Journal of Materials Chemistry*, vol. 21, pp. 18295-18299, 2011.
- [87] M. Wang, Z.-H. Huang, L. Wang, M.-X. Wang, F. Kang and H. Hou, "Electrospun ultrafine carbon fiber webs for electrochemical capacitive desalination," *New Journal of Chemistry*, vol. 34, pp. 1843 - 1845, 2010.
- [88] L. Li, L. Zou, H. Song and G. Morris, "Ordered mesoporous carbons synthesized by a modified sol-gel process for electrosorptive removal of sodium chloride," *Carbon*, vol. 47, pp. 775-781, 2009.
- [89] H. Li, L. Pan, C. Nie, Y. Liu and Z. Sun, "Reduced graphene oxide and activated carbon composites for capacitive deionization," *Journals of Material Chemistry*, vol. 22, pp. 15556 - 155561, 2012.
- [90] D. Zhang, T. Yan, L. Shi, Z. Peng, X. Wen and J. Zhang, "Enhanced capacitive deionization performance of graphene/carbon nanotube composites," *Journal of Materials Chemistry*, vol. 22, p. 14696 – 14704, 2012.
- [91] Z. Peng, D. Zhang, L. Shi and T. Yan, "High performance ordered mesoporous carbon/carbon nanotube composite electrodes for capacitive deionization," *Journal of Materials Chemistry*, vol. 22, p. 6603 – 6612, 2012.
- [92] H. Wang, L. Shi, T. Yan, J. Zhang, Q. Zhong and D. Zhang, "Design of graphene-coated hollow mesoporous carbon spheres as high performance electrodes for capacitive deionization," *Journal of Materials Chemistry A*, vol. 2, pp. 4739 - 4750, 2014.
- [93] P.-I. Liu, L.-C. Chung, H. Shao, T.-M. Liang, R.-Y. Horng, C.-C. M. Ma and M.-C. Chang, "Microwave-assisted ionothermal synthesis of nanostructured

- anatase titanium dioxide/activated carbon composite as electrode material for capacitive deionization," *Electrochimica Acta*, vol. 96, pp. 173-179, 2013.
- [94] C. Yan, L. Zou and R. Short, "Single-walled carbon nanotubes and polyaniline composites for capacitive deionization," *Desalination*, vol. 290, p. 125–129, 2012.
- [95] S. Nadakatti, M. Tendulkar and M. Kadam, "Use of mesoporous conductive carbon black to enhance performance of activated carbon electrodes in capacitive deionization technology," *Desalination*, vol. 268, pp. 182 - 188, 2011.
- [96] S. Porada, L. Weinstein, R. Dash, A. van der Wal, M. Bryjak, Y. Gogotsi and P. M. Biesheuvel, "Water Desalination Using Capacitive Deionization with Microporous Carbon Electrodes," *ACS Applied Materials & Interfaces*, vol. 4, p. 1194–1199, 2012.
- [97] T. Kim and J. Yoon, "CDI Ragone plot as a functional tool to evaluate desalination performance in capacitive deionization," *Royal Society of Chemistry Advances*, vol. 5, p. 1456–1461, 2014.
- [98] Y. Zhang, J. Guo and T. Li, "Research Progress on Binder of Activated Carbon Electrode," *Advanced Materials Research*, vol. 549, pp. 780-784, 2012.
- [99] B. Chen, Y. Wang, Z. Chang, X. Wang, M. Li, X. Liu, L. Zhang and Y. Wu, "Enhanced capacitive desalination of MnO<sub>2</sub> by forming composite with multi-walled carbon nanotubes," *Royal Society of Chemistry Advances*, vol. 6, p. 6730–6736, 2016.
- [100] J. Yang, L. Zou and N. R. Choudhury, "Ion-selective carbon nanotube electrodes in capacitive deionisation," *Electrochimica Acta*, vol. 91, pp. 11 - 19, 2013.

- [101] X. Gu, M. Hu, Z. Du, J. Huang and C. Wang, "Fabrication of mesoporous graphene electrodes with enhanced capacitive deionization," *Electrochimica Acta*, vol. 182, pp. 183 - 191, 2015.
- [102] Z. Li, B. Song, Z. Wu, Z. Lin, Y. Yao, K.-S. Moon and C. P. Wong, "3D porous graphene with ultra high surface area for microscale capacitive deionization," *Nano Energy*, vol. 11, pp. 711 - 718, 2015.
- [103] C. Tsouris, R. Mayes, J. Kiggans, K. Sharma, S. Yiacoumi, D. DePaoli and S. Dai, "Mesoporous Carbon for Capacitive Deionization of Saline Water," *Environmental Science & Technology*, vol. 45, p. 10243–10249, 2011.
- [104] C.-T. Hsieh, D.-Y. Tzou, W.-Y. Lee and J.-P. Hsu, "Deposition of MnO<sub>2</sub> nanoneedles on carbon nanotubes and graphene nanosheets as electrode materials for electrochemical capacitors," *Journal of Alloys and Compounds*, vol. 660, pp. 99 - 107, 2016.
- [105] K. Mohanapriya, G. Ghosh and N. Jha, "Solar light reduced Graphene as high energy density supercapacitor and capacitive deionization electrode," *Electrochimica Acta*, vol. 209, pp. 719 - 729, 2016.
- [106] L. Liu, L. Liao, Q. Meng and B. Cao, "High performance graphene composite microsphere electrodes for capacitive deionisation," *Carbon*, vol. 90, pp. 75 - 84, 2015.
- [107] P.-I. Liu, L.-C. Chung, C.-H. Ho, H. Shao, T.-M. Liang, R.-Y. Horng, M.-C. Chang and C.-C. M. Ma, "Effects of activated carbon characteristics on the electrosorption capacity of titanium dioxide/activated carbon composite electrode materials prepared by a microwave-assisted ionothermal synthesis method," *Journal of Colloid and Interface Science*, vol. 446, pp. 352 - 358, 2015.

- [108] M. E. Suss, T. F. Baumann, W. L. Bourcier, C. M. Spadaccini, K. A. Rose, J. G. Santiago and M. Stadermann, "Capacitive desalination with flow-through electrodes," *Energy & Environmental Science*, vol. 5, p. 9511–9519, 2012.
- [109] W. L. Bourcier, R. D. Aines, J. J. Haslam, C. M. Schaldach, K. C. O'Brein and E. Cussler, "Deionization and Desalination using Electrostatic Ion Pumping". United States (Livermore, CA) Patent 11/655,423, 2011.
- [110] S. Porada, B. B. Sales, H. V. Hamelers and P. M. Biesheuvel, "Water Desalination with Wires," *The Journal of Physical Chemistry Letters*, vol. 3, pp. 1613 - 1618, 2012.
- [111] Y. Oren and A. Soffer, "Graphite felt as an efficient porous electrode for impurity removal and recovery of metals," *Electrochimica Acta*, vol. 28, pp. 1649 - 1654, 1983.
- [112] D. Liu, K. Huang, L. Xie and H. L. Tang, "Relation between operating parameters and desalination performance of capacitive deionization with activated carbon electrodes," *Environmental Science: Water Research & Technology*, vol. 1, pp. 516 - 522, 2015.
- [113] R. L. Zornitta, J. J. Lado, M. A. Anderson and L. A. Ruotolo, "Effect of electrode properties and operational parameters on capacitive deionization using low-cost commercial carbons," *Separation and Purification Technology*, vol. 158, pp. 39-52, 2016.
- [114] Y. Zhao, X.-m. Hu, B.-h. Jiang and L. Li, "Optimization of the operational parameters for desalination with response surface methodology during a capacitive deionization process," *Desalination*, vol. 336, pp. 64 - 71, 2014.
- [115] C. Wang, H. Song, Q. Zhang, B. Wang and A. Li, "Parameter optimization based on capacitive deionization for highly efficient desalination of domestic

- wastewater biotreated effluent and the fouled electrode regeneration," *Desalination*, vol. 365, pp. 407 - 415, 2015.
- [116] M. Mossad and L. Zou, "A study of the capacitive deionisation performance under various operational conditions," *Journal of Hazardous Materials*, Vols. 213-214, pp. 491 - 497, 2012.
- [117] C. Huyskens, J. Helsen and A. B. de Haan, "Capacitive deionization for water treatment: Screening of key performance parameters and comparison of performance for different ions," *Huyskens*, vol. 328, pp. 8-16, 2013.
- [118] T.-C. Chung, *Evaluating the Desalination Performance and Efficiency of Capacitive Deionization with Activated Carbon Electrodes* (Master's thesis), 2018.
- [119] C. J. Gabelich, T. D. Tran and I. H. Suffet, "Electrosorption of Inorganic Salts from Aqueous Solution Using Carbon Aerogels," *Environmental Science & Technology*, vol. 36, pp. 3010-3019, 2002.
- [120] P. Xu, J. E. Drewes, D. Heil and G. Wang, "Treatment of brackish produced water using carbon aerogel-based capacitive deionization technology," *Water Research*, vol. 42, p. 2605 – 2617, 2008.
- [121] Y. Gao, L. Pan, H. Li, Y. Zhang, Z. Zhang, Y. Chen and Z. Sun, "Electrosorption behavior of cations with carbon nanotubes and carbon nanofibres composite film electrodes," *Thin Solid Films*, vol. 517, no. 5, pp. 1616-1619, 2009.
- [122] E. Frackowiak and F. Beguin, "Carbon materials for the electrochemical storage of energy in capacitors," *Carbon*, vol. 39, p. 937–950, 2001.
- [123] S. Ban, J. Zhang, L. Zhang, K. Tsay, D. Song and X. Zou, "Charging and discharging electrochemical supercapacitors in the presence of both parallel

leakage process and electrochemical decomposition of solvent," *Electrochimica Acta*, vol. 90, pp. 542-549, 2013.

- [124] M. D. Stoller and R. S. Ruoff, "Best practice methods for determining an electrode material's performance for ultracapacitors," *Energy & Environmental Science*, vol. 3, pp. 1294 - 1301, 2010.
- [125] C.-H. Hou and C.-Y. Huang, "A comparative study of electrosorption selectivity of ions by activated carbon electrodes in capacitive deionization," *Desalination*, vol. 314, pp. 124-129, 2013.
- [126] M. Naebe, J. Wang, A. Amini, H. Khayyam, N. Hameed, L. H. Li, Y. Chen and B. Fox, "Mechanical Property and Structure of Covalent Functionalised Graphene/Epoxy Nanocomposites," *Scientific Reports*, vol. 4, 2014.
- [127] B. Andonovic, A. Ademi, A. Grozdanov, P. Paunović and A. T. Dimitrov, "Enhanced model for determining the number of graphene layers and their distribution from X-ray diffraction data," *Beilstein Journal of Nanotechnology*, vol. 6, p. 2113–2122, 2015.
- [128] G. Wang, C. Pan, L. Wang, Q. Dong, C. Yu, Z. Zhao and J. Qiu, "Activated carbon nanofiber webs made by electrospinning for capacitive deionization," *Electrochimica Acta*, vol. 69, pp. 65 - 70, 2012.
- [129] A. C. Ferrari, "Raman spectroscopy of graphene and graphite: Disorder, electron–phonon coupling, doping and nonadiabatic effects," *Solid State Communications*, vol. 143, pp. 47 - 57, 2007.
- [130] M. A. A. Shahmirzadi, S. S. Hosseini, J. Luo and I. Ortiz, "Significance, evolution and recent advances in adsorption technology, materials and processes for desalination, water softening and salt removal," *Journal of Environmental Management*, vol. 215, pp. 324 - 344, 2018.

- [131] J. J. Lado, R. E. Pérez-Roa, J. J. Wouters, M. I. Tejedor-Tejedor, C. Federspill and M. A. Anderson, "Continuous cycling of an asymmetric capacitive deionization system: An evaluation of the electrode performance and stability," *Journal of Environmental Chemical Engineering*, vol. 3, pp. 2358 - 2367, 2015.
- [132] S. Yoon, J. Lee, T. Hyeon and S. M. Oh, "Electric Double-Layer Capacitor Performance of a New Mesoporous Carbon," *Journal of The Electrochemical Society*, vol. 147, no. 7, pp. 2507 - 2512, 2000.
- [133] D. Zhang , X. Wen , L. Shi , T. Yan and J. Zhang , "Enhanced capacitive deionization of graphene/mesoporous carbon composites," *Nanoscale*, vol. 4, pp. 5440 - 5446, 2012.